

# 1. LEG 202 SYNTHESIS: SOUTHEAST PACIFIC PALEOCEANOGRAPHY<sup>1</sup>

Ralf Tiedemann<sup>2</sup> and Alan Mix<sup>3</sup>

## ABSTRACT

Ocean Drilling Program (ODP) Leg 202 has opened a new window into understanding late Paleogene and Neogene global environmental change by providing high-quality sediment sequences from a previously unsampled region, the eastern South Pacific. Eleven sites (1232–1242) that record variations on timescales ranging from decades to tens of millions of years were drilled and investigated on transects of both depth (489–4072 m) and latitude (41°S–8°N). Building on the shipboard results presented in the Leg 202 *Initial Reports* volume, postcruise research has significantly improved the stratigraphic framework and provided new insights into climate-related processes, which operate on different timescales and are relevant to hypotheses concerning the bipolar “see-saw” climate mechanism, orbitally driven changes in the continent-ocean-ice-atmosphere system and tectonic processes associated with the uplift of the Andes, closure of the Central American Seaway, and major expansions of polar ice sheets.

Stable isotope records and refinements in bio- and magnetostratigraphy in combination with orbitally tuned cyclostratigraphy significantly improved the Pleistocene stratigraphy at Sites 1233 and 1234, the Miocene–Pliocene stratigraphy at Sites 1236, 1237, 1239, and 1241, and the Oligocene stratigraphy around the late Oligocene climate optimum at Site 1237. Site 1233 filled a crucial gap in the stratigraphic and paleoceanographic archive of the South Pacific sector of the Southern Ocean by providing an outstanding reproducible accelerator mass spectrometry (AMS) <sup>14</sup>C-dated paleomagnetic record of centennial- and millennial-scale variability, representing regional variations in environmental/climatic conditions for the past 70,000 yr. With regard to the Cenozoic timetable, the continuous and complete sedimentary

<sup>1</sup>Tiedemann, R., and Mix, A., 2007. Leg 202 synthesis: southeast Pacific paleoceanography. In Tiedemann, R., Mix, A.C., Richter, C., and Ruddiman, W.F. (Eds.), *Proc. ODP, Sci. Results*, 202: College Station, TX (Ocean Drilling Program), 1–56. doi:10.2973/odp.proc.sr.202.201.2007

<sup>2</sup>Alfred Wegener Institute for Polar and Marine Research, Section Marine Geology and Paleontology, Columbusstrasse, D-27568 Bremerhaven, Germany.

[rtiedemann@awi-bremerhaven.de](mailto:rtiedemann@awi-bremerhaven.de)

<sup>3</sup>College of Oceanic and Atmospheric Sciences, COAS Administration Building 104, Oregon State University, Corvallis OR 97331-5503, USA.

Initial receipt: 14 June 2006

Acceptance: 12 February 2007

Web publication: 20 March 2007

Ms 202SR-201

sequence of Site 1237, spanning the last ~31 m.y., has the potential of becoming a stratigraphic reference section for the South Pacific. Post-cruise work demonstrated the excellence of this record for producing a stratigraphic framework that combines the biostratigraphy and terrific magnetostratigraphy with orbitally tuned stable isotope records.

With respect to the bipolar see-saw hypotheses, Leg 202 studies on high-resolution records changed the view of the global distribution of millennial-scale climate change. These studies clearly demonstrate that millennial-scale climate and biogeochemical systems of the southeast Pacific and Chile closely align with those recorded in Antarctica and the southern oceans and that these climate patterns extend to the equatorial Pacific, either transmitted directly by the eastern boundary current or indirectly by “the oceanic tunnel” (subsurface transport via Antarctic Mode or Intermediate Water, Equatorial Undercurrent) injecting Southern Hemisphere extratropical water masses into the equatorial upwelling system.

On orbital timescales, most spectacular was the finding that Earth’s final transition into an “icehouse” climate ~13.9 m.y. ago, the middle Miocene intensification of Antarctic glaciation, coincided with a striking transition from obliquity to eccentricity as the drivers of climate change. Thus, the late Pleistocene 100-k.y. climate cycles are not unique in Earth’s history, and although the examples from the Miocene and Pleistocene are both associated with climate cooling, they occur under significantly different global boundary conditions. This important contribution from Leg 202 issues a challenge to climatologists to understand multiple origins of 100-k.y. climate cycles that are now well documented in the geologic record.

On timescales of millions of years, late Neogene upper ocean temperature reconstructions in combination with salinity assessments at selected sites from Leg 202 provide further insights into the reorganization of ocean-atmosphere couplings that are linked to the shoaling of the Central American Seaway (CAS), uplift of the Andes, and Pliocene amplification of polar ice sheet expansion. Regional shoaling of the thermocline in the low-latitude eastern Pacific from 5.3 to 4.0 Ma most likely resulted from shoaling of the CAS, as suggested by model experiments. Mixed-layer cooling and freshening in the tropical northeast Pacific warm pool as well as declining sea-surface temperature (SST) and increasing biological productivity off Chile parallel intensification of Northern Hemisphere glaciation from 3.6 to 2.4 Ma. The similarity of temporal changes in SST, upwelling, and dust flux between the Benguela and Chile upwelling systems suggests that uplift of the Andes was probably of secondary importance for generating the observed changes in the southeast Pacific within the last 6 m.y., as the Benguela upwelling system was not affected by mountain uplift. The expected atmosphere-oceanic response of the southeast Pacific to uplift of the Andes probably played a larger role during the late Miocene, prior to 6 Ma.

A particular scientific challenge of future Leg 202 paleoclimate research is to better understand the transitions between these different timescales with respect to couplings between global, regional, and local processes.

## INTRODUCTION

Ocean Drilling Program (ODP) Leg 202 was designed to study the timing, nature, and processes of late Cenozoic climatic and oceanographic changes in the southeast Pacific. During Leg 202, we recovered a total of 7081 m of sediment at 11 sites (Sites 1232–1241) in the southeast and equatorial Pacific, ranging in age from early Oligocene (~31.5 Ma) to Holocene (Figs. F1, F2, F3). At all sites, multiple holes were drilled to ensure continuous recovery of the stratigraphic section. At three sites (1238, 1239, and 1241), borehole logging operations produced data sets of remarkable quality, which allowed core-log integration. A complete description of Leg 202 recovered sediments and performed shipboard analyses is given in the Leg 202 *Initial Reports* volume (Mix, Tiedemann, Blum, et al., 2003). We successfully achieved the drilling goal of providing undisturbed and continuous sediment records along a latitudinal transect from 41°S to 8°N and an intermediate- to deepwater transect from 490 to 4070 m water depth that permit paleoceanographic studies on a variety of timescales, including centennial to millennial ( $10^2$ – $10^3$  yr), orbital ( $10^4$ – $10^5$  yr), and tectonic ( $>10^5$  yr) time resolution.

These materials provide an excellent opportunity to test a broad set of hypothesis on

1. The evolution of the South Pacific Ocean as it responds to and modulates the effects of major tectonic and climatic events, such as uplift of the Andes Mountains, closure of the CAS, and major expansion of polar ice sheets;
2. The linkage between climate and biogeochemical changes in the high latitudes and the equatorial Pacific, related to rhythmic changes in Earth's orbit, and the relationship of such changes to well-known glacial events of the Northern Hemisphere; and
3. The timing of global and regional changes in climate, biota, and ocean chemistry on scales of centuries to millennia.

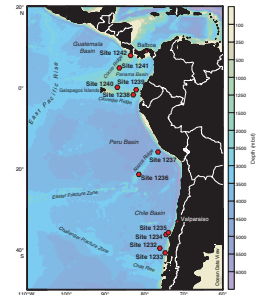
Four years of postcruise work have yielded substantial progress. Here we present a summary of Leg 202 state-of-the-art science by (1) providing an overview of the papers that contributed to this *Scientific Results* volume and (2) synthesizing the reports both in the volume and in the external literature, and (3) evaluating the current state of progress toward meeting the overall leg objectives, recognizing that ongoing and future efforts will continue to capitalize on these extraordinary materials and add to these results over the coming decades.

## OVERVIEW OF POSTCRUISE PUBLICATIONS

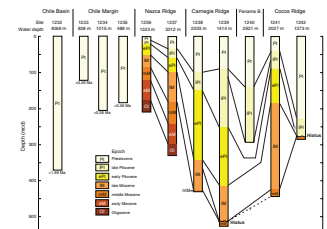
Fourteen papers appearing in this volume and sixteen papers published outside the Leg 202 *Scientific Results* volume add significant information about stratigraphy, continent-ocean-atmosphere couplings, and associated biogeochemical interactions on a variety of timescales and with different temporal resolutions. These contributions are briefly summarized below.

Abe et al. (this volume) provide a data report on Miocene to Holocene organic carbon and biomarker variations at Sites 1237 and 1239. Concentrations of organic carbon, carbonate, long-chain *n*-alkanes, and

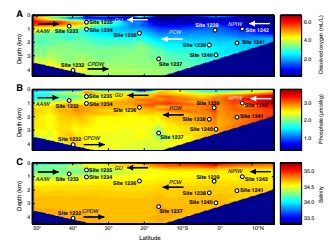
F1. Site locations of Leg 202, p. 41.



F2. Summary stratigraphic columns, p. 42.



F3. Subsurface water masses: dissolved oxygen, dissolved phosphate, and salinity, p. 43.



total alkenones, as well as alkenone-based sea-surface temperature (SST) estimates are presented. The geochemical data can be used to evaluate terrestrial sediment sources. Reconstruction of sea-surface temperatures suggests a significant temperature drop at both sites after ~2.5 Ma, possibly in response to the intensification of Northern Hemisphere glaciation (NHG). The range of temperature variability (~7°–8°C in this low-resolution data set from Site 1237) is generally consistent with alkenone temperatures reconstructed for the late Pleistocene at a nearby piston core (Calvo et al., 2001; Prah1 et al., 2006), with alkenone temperature shifts between the late Pleistocene and mid-Pliocene warm period (3.0–3.3 Ma) at Site 1237 (Haywood et al., 2005), but conflicts with Mg/Ca temperature reconstructions of [Wara and Ravelo](#) (this volume), which suggest no significant long-term temperature changes over the past ~6 m.y. For comparison, long-term variations of alkenone temperature estimates in the equatorial cold tongue (Site 846; Lawrence et al., 2006) also document a temperature range of ~7°C, although unlike the data from Site 1237, changes at Site 846 include a long-term “ramp” of cooling over the past 5 m.y. superimposed on shorter-term variations.

Abrantes et al. (2007) use core-top samples from throughout the region of Leg 202 to develop transfer functions for quantitatively predicting mean annual SST and primary productivity and qualitatively assessing freshwater input to the marine realm, based on fossil diatom assemblages. This calibration of paleoproxies with careful regional studies of modern sediments provides an important step toward future quantification of oceanographic change in the downcore records.

Benway and Mix (2004) provide oxygen isotope and salinity data on seawater and rainwater sampled during Leg 202 in the eastern tropical Pacific region, providing a basis for reconstructing paleosalinity from estimates of  $\delta^{18}\text{O}$  in seawater. Based on an isotope balance, they suggest that about half of the rainfall in the Panama Bight comes from local evaporation and precipitation and the other half comes from long-distance, cross-isthmus transport and intermittent large storm events.

Benway et al. (2006) provide high-resolution  $\delta^{18}\text{O}$  and Mg/Ca data on planktonic foraminifers from Site 1242 and other sediment cores and reconstruct substantial millennial-scale changes (but little glacial–interglacial difference) in  $\delta^{18}\text{O}$  of seawater (and, by inference, upper ocean salinity, corrected for sea level change) that are significantly larger than those of the Caribbean (Schmidt et al., 2004). Such variations likely reflect the combination of changing location of the intertropical convergence and changes in net freshwater transport across the Panama Isthmus. Surprisingly, millennial-scale changes in freshwater transport across the Panama Isthmus appear to lead millennial-scale changes in thermohaline overturn in the North Atlantic region, suggesting an active role for the tropics in generating such variations, either as an independent tropical trigger or as part of an integrated feedback loop between the tropical and high-latitude climate systems.

[Chun and Delaney](#) (this volume) present a detailed examination of particulate phosphorus composition, biogenic barium, manganese, and uranium at Site 1237 in order to characterize the history of nutrient burial and paleoproductivity in the context of major tectonic and climate changes during the past 31 m.y. A stepwise decrease in manganese enrichment observed near 162 meters composite depth (mcd), or ~9 Ma, is consistent with a redox threshold associated with expected increases in paleoproductivity as tectonic drift carried the site under the eastern boundary current system off western South America (Mix, Tiedemann, Blum, et al., 2003).

Flores et al. (this volume) provide a data report that significantly improves the Pleistocene calcareous nannofossil biostratigraphy at Sites 1237, 1238, 1241, and 1242. They confined 11 events of key biostratigraphic marker species (e.g., first occurrence [FO] and last occurrence [LO] datums) using a sampling resolution of 10–30 cm for the last 0.5 m.y. and 75–150 cm for the time interval from 0.5 to 2.0 Ma.

Flower and Chisholm (this volume) present a late Oligocene stable isotope record (*Cibicidoides mundulus*) from deepwater Site 1237 and tie the onset of the late Oligocene climate optimum to the new geologic timescale (GTS 2004) (Gradstein et al., 2004) by using magnetic polarity stratigraphy and isotope data. Their results suggest an age of 26.35 Ma for the final decrease in  $\delta^{18}\text{O}$ , marking the initiation of the late Oligocene climate optimum. This climatic shift is closely associated with the LO of the planktonic foraminifer *Paragloborotalia opima*.

Grevemeyer et al. (2003) examine the thermal regime of the continental slope and downgoing slab in Chile between 32° and 41°S by combining information from seismic reflection data (Empresa Nacional del Petroleo Chilean oil company and Bundesministerium für Bildung und Wissenschaft, Germany) and downhole temperature measurements obtained during Leg 202 at Sites 1233, 1234, and 1235. Their results suggest that the heat flow through the upper Nazca plate is low with respect to the Eocene age of the incoming oceanic lithosphere. Modeling shows that reduced heat flow can be accounted for by the fact that the downgoing Nazca plate advects heat into the mantle and hence acts as heat sink. The occurrence of bottom simulating reflectors (BSRs) is interpreted to mark the thermally controlled base of gas hydrate layers. BSR heat flow over the accretionary prism is 60%–80% of the regional conductive model and is suggested to reflect the initial thickening of sediment as it is being incorporated into the accretionary wedge. Heat flow over continental basement rocks, however, is generally in accordance with the regional model and may reflect steady-state conditions. The seaward limit of the seismogenic zone is characterized by the 100°C isotherm and occurs 60 km landward of the trench axis in the north (33°S) and 30 km landward in the south. The seaward shift is related to the subduction of younger lithosphere in the south.

Groeneveld et al. (this volume) present high-resolution Pliocene Mg/Ca and  $\delta^{18}\text{O}$  records from tropical east Pacific Site 1241 that were both measured on the planktonic mixed-layer species *Globigerinoides sacculifer*. Their results suggest a freshening of the mixed layer from 4.8 to 2.4 Ma, which might be coupled with progressive closure of the CAS. Mixed-layer temperatures commenced to decrease after 3.7 Ma, paralleling the Pliocene intensification of NHG that started at ~3.6 Ma, according to the recent work of Mudelsee and Raymo (2005). Groeneveld et al. note, however, that Pliocene SSTs at Site 1241 are similar to modern values and colder than values estimated for the western Pacific warm pool, providing no direct support for the idea of permanent El-Niño conditions during the early Pliocene (Ravelo et al., 2006).

Haywood et al. (2005) present new estimates of mid-Pliocene Pacific SSTs from subtropical Site 1237 using alkenone paleothermometry. These estimates, combined with other SST data from the Pacific and Atlantic, were used to verify model-predicted and fossil-based temperature estimates in the PRISM2 data set that was produced by the Pliocene Research Interpretations and Synoptic Mapping (PRISM) Group. The PRISM Group suggested that mid-Pliocene surface ocean temperatures were the same as, or slightly cooler than, those found today in the tropics and at low latitudes and significantly warmer at higher latitudes.

This change in the latitudinal pattern of SSTs has been attributed to enhanced meridional ocean heat transport generated by more vigorous surface ocean gyres and/or thermohaline circulation. In contrast, alkenone and model-based SST estimates of Haywood et al. (2005) suggest warmer SSTs during the mid-Pliocene in the tropics and subtropics. This pattern of SSTs is not characteristic of that produced by enhanced meridional ocean heat transport or thermohaline circulation. Instead, the pattern is similar to that which might be expected as a result of higher concentrations of atmospheric CO<sub>2</sub>, which would act to warm the oceans at the tropics and other latitudes. Furthermore, model diagnostics indicate that reduced sea ice and terrestrial ice sheet extent as well as a strong ice-albedo feedback played a major role in forcing mid-Pliocene warmth.

Heusser et al. (2006b) compile high-resolution pollen records from Site 1233, providing a continuous, chronostratigraphically controlled 50-k.y. record of regional changes in vegetation from temperate South America. Deposited 38 km west of the transition from northern deciduous lowland forest to southern evergreen rain forest, the pollen record documents the comparatively brief Holocene development of thermophilous vegetation (Lowland Deciduous Beech Forest and Valdivian Evergreen Forest) and the expansion of glacial subantarctic vegetation (North Patagonian Evergreen Forest–Subantarctic Parkland) during marine isotope Stages (MIS) 2 and 3. Systematic variability in these terrestrial climate proxies, which reflect latitudinal movement of the southern westerlies, is mirrored in Antarctic climate records and in coeval ocean conditions inferred from radiolarian census data (Pisias et al., 2006).

Heusser et al. (2006a) present joint pollen and benthic oxygen isotope data from Site 1234 in the southeast Pacific. Their data provide the first continuous, chronostratigraphically controlled record of changes in temperate South American vegetation and climate for the last 140 k.y. Downhole changes in diagnostic pollen assemblages from xeric lowland deciduous forest, mesic Valdivian Evergreen, and Subantarctic Evergreen Rainforest reveal large rapid shifts that likely reflect latitudinal movements in atmospheric circulation and storm tracks associated with the southern westerly winds. During glacial maxima (MIS 2–4 and 6), the prominence of hyperhumid vegetation (north Patagonian and subantarctic forests and parkland) implies sustained northward migration of the southern westerlies. At the MIS 6/5e boundary, coeval with the rapid shift to lower isotopic values, rainforest vegetation was rapidly replaced by xeric plant communities associated with Mediterranean-type climate. An increased prominence of halophytic vegetation suggests that MIS 5e was more arid and possibly warmer than MIS 1. Although rainforest pollen rises again at the end of MIS 5e, lowland deciduous forest pollen persists through MIS 5d and 5c, into MIS 5b. Comparison to Antarctic ice core data suggests that glacial–interglacial advances of the Chilean rainforests occurred in phase with Antarctic cooling. On millennial scales, changes in vegetation lag Antarctic temperature change, suggesting that southern Chilean ecosystems respond to regional climate change with an exponential response time of ~1000 yr.

Holbourn et al. (2005) develop an orbitally tuned age model for the middle Miocene time interval from 12.7 to 14.7 Ma at Site 1237 and examine the impacts of orbital forcing and atmospheric CO<sub>2</sub> on Miocene Antarctic ice sheet expansion. Their studies are based on benthic foraminiferal oxygen and carbon isotope (4- to 5-k.y. resolution) and X-ray fluorescence (XRF) scanning records (1-k.y. resolution). The new chro-

nology was generated by initially matching 400- and 100-k.y. amplitude variations in the benthic  $\delta^{18}\text{O}$  record to the latest astronomical solution of Laskar et al. (2004) and then fine-tuning obliquity-related  $\delta^{18}\text{O}$  cycles to the orbital record. The major increase in mid-Miocene ice sheet expansion at 13.91–13.84 Ma was marked by a striking transition from high-amplitude 41-k.y.-paced  $\delta^{18}\text{O}$  variations (prior to 13.9 Ma) to high-amplitude 100-k.y.-paced variations, which are paralleled by a similar shift in the amplitudes of orbital obliquity and eccentricity. The major steps of rapid ice sheet expansion occurred during an extended interval of low seasonal contrast at low eccentricity and coincided with a prominent increase in benthic  $\delta^{13}\text{C}$  that was interpreted as reflecting a decrease in atmospheric  $\text{CO}_2$  contents, promoting global cooling.

Hostetler et al. (2006) assemble available SST data (modern and Last Glacial Maximum [LGM]) from the tropical and subtropical Pacific (including data from Sites 1233 and 1242) and apply a statistical approach to adjust hypothesized biases in the faunal based SST estimates of the Climatic Long-Range Investigation, Mapping, and Prediction Project (CLIMAP Project Members, 1981). The resulting SSTs are generally in better agreement than CLIMAP with recent geochemical estimates of glacial–interglacial temperature changes. In addition, they conduct a series of model experiments using the GENESIS (Global Environmental and Ecological Simulation of Interactive Systems) general atmospheric circulation model to assess the sensitivity of the climate system to their bias-adjusted SSTs. Globally, the new SST field results in a modeled LGM cooling of 6.4°C (1.9°C cooler than that of CLIMAP). Data model comparisons indicate improvement in agreement relative to CLIMAP, but differences among terrestrial data inferences and simulated moisture and temperature remain. Their SSTs result in positive mass balance over the Northern Hemisphere ice sheets (primarily through reduced summer ablation), supporting the hypothesis that tropical and subtropical ocean temperatures may have played a role in triggering glacial changes at higher latitudes.

Kaiser et al. (2005) extend the alkenone-derived SST record at Site 1233 (Lamy et al., 2004) back to 70 ka. Comparison to other mid-latitude Southern Hemisphere records suggests that the Antarctic timing of SST changes was probably a hemisphere-wide phenomenon. Gradient reconstructions of SSTs over the complete latitudinal range of the Pacific eastern boundary current system suggest a displaced subtropical gyre circulation toward the Equator during glacial MIS 2 and 4.

Kaiser et al. (in press) provide a continuous record of Patagonian ice sheet (PIS) extent (Fe content) and alkenone-based SSTs off Chile during the last 70 k.y. based on Site 1233. In particular, they focus on the millennial- to multicentennial-scale variability of the paleorecords. The close relationship between Fe content and SST pattern in the southeast Pacific (as described by Lamy et al. [2004] for the 50- to 19-k.y. time interval) extends into the older part of the records (70–50 ka). During MIS 4, a delay of ~500 yr of PIS retreats relative to SST increases has been found, similar to that described for the coldest part of MIS 3 and 2. During early MIS 3 (~60–56 ka), synchronous variability in both records resembles the deglacial–Holocene time interval, reflecting either a meltwater pulse or dominant control of Fe input by rainfall changes related to a rather small PIS. Results of spectral analysis on the detrended records show three main periodicity bands at ~4.5–3.1, 2.4–2.2, and 1.2–1 ka. The possible origins of these bands are discussed in terms of

stochastic resonance, solar forcing, and Northern Hemisphere high- and/or low-latitude influences on the southeast Pacific, respectively.

Lamy et al. (2004) establish alkenone-derived SST, planktonic  $\delta^{18}\text{O}$ , and Fe (XRF scanning) records at the Chilean continental margin Site 1233 and reconstruct millennial-scale changes in southeast Pacific surface water properties and PIS extent for the last 50 k.y. Their results suggest a clear Antarctic timing of SST changes, which appear to be systematically linked to meridional displacements in sea ice, westerly winds, and the circumpolar current system. The changing Fe contents have been related to glaciofluvial sediment flux from the Andes to the continental margin. The patterns of Fe and paleotemperature records are very similar, but Fe changes lag variations in temperature by as long as ~1000 yr. This was interpreted as reflecting the glacier response time to rising SSTs and may explain some of the current discrepancies among terrestrial records in southern South America.

**Lund et al.** (this volume a) compare detailed rock magnetic and paleomagnetic records of the same age but from different holes of Site 1233 in order to assess whether this late Pleistocene–Holocene archive, deposited at extremely high accumulation rates, contains reproducible evidence for centennial-scale environmental, climatic, and geomagnetic field variability. Their rock magnetic results identify reproducible, pervasive, and distinctive centennial- (~150–300 yr) and millennial-scale variability, representing regional variations in environmental or climate conditions.

**Lund et al.** (this volume b) summarize the complete paleomagnetic record from Site 1233 and the paleomagnetic record for the uppermost 30 mcd from Site 1234. Their study identifies reproducible high-resolution records of paleomagnetic secular variation, which can be correlated between the two sites. These records provide evidence for three magnetic field excursions. On the basis of high-resolution accelerator mass spectrometry (AMS) radiocarbon stratigraphy, two of these excursions occurred at ~35,000 calendar years before present (cal. yr BP) and the third at ~41,000 cal. yr BP.

Martinez et al. (2006) report a nitrogen isotope record of bulk organic matter from southern Chile margin Site 1233. The site is located slightly south of the Peru-Chile upwelling system and the associated oxygen minimum zone. The  $\delta^{15}\text{N}$  values at Site 1233 are relatively high throughout the record, varying between 9‰ and 13‰ during the last 50 k.y. The major features are a pronounced  $\delta^{15}\text{N}$  increase at the beginning of the deglaciation (~19.5 ka), a large decrease during the early Holocene after 10 ka, and a pattern of millennial-scale variability that resembles the pattern of Antarctic climate change as recorded in the  $\delta^{18}\text{O}$  Byrd ice core record. The timing of changes in  $\delta^{15}\text{N}$  appears to be synchronous with Antarctic climate changes between 50 and 10 ka. The Holocene drop in  $\delta^{15}\text{N}$  is a typical feature of Southern Ocean sites, as suggested by comparisons with other  $\delta^{15}\text{N}$  records. The authors propose that the interplay between nutrient demand in the Subantarctic Zone and latitudinal shifts of hydrologic fronts controlled both the concentrations and the isotopic signature of the remaining nitrate delivered to the Chile margin. At that time the glacial surface waters of the southern Chile margin were likely lower in nitrate concentration and higher in  $\delta^{15}\text{N}$  than during interglacial periods.

**McManus** (this volume) provides a data report on major (K, Ca, Mg, Fe, and Ti) and trace (Mn, Cu, Ba, U, Cd, Mo, and V) element concentrations at Sites 1233 and 1234 as background for assessing terrigenous

inputs and changes in the reducing nature of these sediments from the Chilean continental margin. In particular, the ratio U/Mo may provide a linear measure of bottom water oxygen concentration, with relatively little local impact from diagenesis of organic matter within the sediment. Preliminary application of this new proxy to Sites 1233 and 1234 is consistent with modern bottom water gradients but suggests substantial variability of the oxygen minimum zone, which overlies Site 1233.

Pena et al. (2005) analyze the geochemical composition of foraminifer shells from Site 1240 (Panama Basin) with several analytical techniques (laser ablation inductively coupled plasma–mass spectroscopy [LA-ICP-MS], ICP-MS, X-ray diffraction [XRD], scanning electron microscopy [SEM], and energy dispersive X-ray [EDX]) in order to identify and evaluate the occurrence of contaminant phases that may bias paleoenvironmental reconstructions. LA-ICP-MS results on uncleaned tests indicate the presence of Mn-Mg-rich contaminant phases at the inner surfaces of the foraminiferal shells. Different cleaning techniques were applied to remove these contaminant phases. Satisfactory results were only produced when a reductive step was included. XRD analysis further revealed that the Mn-Mg-rich phase represents the Ca-Mn-Mg carbonate kutnahorite ( $\text{Ca}[\text{Mn},\text{Mg}][\text{CO}_3]_2$ ). Their results demonstrate that the presence of kutnahorite-like minerals can bias Mg/Ca ratios toward higher values (by 7%–36%) and lead to significant overestimation of past seawater temperatures.

Pisias et al. (2006) accomplish multivariate statistical analyses on late Pleistocene–Holocene radiolarian and pollen populations from Chilean continental margin Site 1233. Their sampling intervals yield a temporal resolution of 200–400 yr and provide a detailed record of marine and continental climate change in the southeast Pacific and South American continent for the past 50 k.y. The authors concluded the following:

1. During the past 50 k.y., the region of the central Chilean coast was not directly influenced by polar water from the Antarctic region;
2. Changes in ocean conditions off central Chile during this time interval primarily reflect north–south shifts in the position of the South Pacific transition zone;
3. Changes in Chilean vegetation reflect comparable latitudinal shifts in precipitation and the position of the southern westerlies;
4. The first canonical variate of radiolarian and pollen records extracted from Site 1233 are remarkably similar to each other as well as to temperature records from the Antarctic, which suggests that marine and continental climate variability in the region is tightly coupled at periods longer than 3000 yr; and
5. Phase coupling of these climate records, which leads to variations of continental erosion based on iron abundance at the same site, is consistent with the hypothesis that erosion is linked to relatively long response times (i.e., a few thousand years) of the PIS and thus is not a direct indicator of regional climate.

**Prokopenko et al.** (this volume) compare ammonium and total nitrogen concentrations as well as nitrogen isotope composition of solid phase and dissolved pore water ammonium from Pleistocene sediments that accumulated rapidly at continental margin Sites 1234, 1235, and 1238 and discuss the impact of diagenesis on the  $\delta^{15}\text{N}$  preserved in organic matter. Their results suggest that the  $\delta^{15}\text{N}$  composition of organic matter at Sites 1234 and 1235 is not significantly affected by diagenesis, even though ~20% of organic nitrogen is lost to diagenesis. This is indi-

cated by the strong similarity between  $\delta^{15}\text{N}$  of ammonium and  $\delta^{15}\text{N}$  of organic matter, which implies that the process of organic matter decomposition is not associated with an intrinsic fractionation factor.

Robinson et al. (2007) generate high-resolution oxygen isotope and bulk sediment  $^{15}\text{N}/^{14}\text{N}$  records (Site 1234) in order to assess denitrification changes within the Peru-Chile upwelling system over the last ~70 k.y. Denitrification changes at Chilean margin Site 1234 are coherent with Antarctic climate changes recorded by the Byrd ice core  $\delta^{18}\text{O}$  record rather than with Northern Hemisphere climate change. The Southern Hemisphere character of the Chile margin  $\delta^{15}\text{N}$  record suggests that episodes of reduced denitrification in the eastern Pacific represent times when more oxygen was supplied as the result of changes in the chemical composition of Subantarctic Mode Water (SAMW), which forms in the Subantarctic Zone of the Southern Ocean and ventilates the low-latitude thermocline.

**Steph et al.** (this volume) provide Pliocene Mg/Ca temperature and stable isotope records from shallow- and deep-dwelling planktonic foraminifers (Site 1241) that span the time interval from 5.5 to 2.5 Ma. The combination of paired Mg/Ca and  $\delta^{18}\text{O}$  measurements allowed them to differentiate between temperature and salinity changes and therefore assess changes in upper ocean stratification. Their study indicates an early Pliocene shoaling of the tropical east Pacific thermocline, marked by a  $6^\circ\text{C}$  temperature decrease at the bottom of the photic zone between 5.4 and 4.0 Ma. The deviation of  $\delta^{18}\text{O}$  records and Mg/Ca temperature estimates from thermocline-dwelling planktonic foraminifers suggests that local changes in salinity exerted a much stronger control on Pliocene tropical east Pacific upper ocean water mass signatures than previously assumed. Whether these variations are triggered by changes in the configuration of low-latitude ocean gateways is being discussed.

Steph et al. (2006) compare Pliocene  $\delta^{18}\text{O}$  records of shallow- and deep-dwelling planktonic foraminifers from the tropical east Pacific (Sites 1241 and 851), Caribbean (ODP Sites 999 and 1000), and Atlantic (Site 925, Ceara Rise, and Site 1006, western Great Bahama Bank) to assess Atlantic-Caribbean-Pacific atmospheric and oceanic linkages associated with progressive closure of the CAS. Comparisons suggest development of an inner-Caribbean salinity gradient in the mixed layer and salinity changes on precessional periodicities after 4.4 Ma (Site 1000) when Pacific-Caribbean throughflow became significantly restricted. Precession-induced variations in the volume transport of Pacific surface water masses through the Panamanian Seaway are considered a main factor to explain the Caribbean salinity minima. Results from a coupled climate model point to changes in the El Niño Southern Oscillation (ENSO) state as a potential trigger for changes in the amount of Pacific inflow into the Caribbean.

**Tiedemann et al.** (this volume) present consistent high-resolution, orbitally tuned age models for Sites 1237 and 1241 as well as benthic  $\delta^{18}\text{O}$  and  $\delta^{13}\text{C}$  stratigraphies for Sites 1236, 1237, 1239, and 1241, which cover the time interval from 2.5 to 6 Ma. The age models for Sites 1237 and 1241 were generated by correlating the high-frequency variations in gamma ray attenuation (GRA) density, sand percentages of the carbonate fraction, and benthic  $\delta^{13}\text{C}$  to the orbital solution of Laskar et al. (1993). The tuned ages of the Pliocene polarity reversals at Site 1237 agree well with those of GTS 2004 (Gradstein et al., 2004).

**Wara and Ravelo** (this volume) present a data report on geochemical analyses performed on planktonic and benthic foraminifers from

Site 1237. Records of planktonic and benthic  $\delta^{18}\text{O}$  and  $\delta^{13}\text{C}$  as well as planktonic Mg/Ca, Sr/Ca, and Mn/Ca concentrations were generated for the time interval of the last 6 m.y. to provide critical information regarding the late Miocene to present history of climate and oceanographic variability in the southeast Pacific. These records can be used to infer changes in SST and salinity.

**Weber and Pisas** (this volume) provide an initial radiolarian biostratigraphic framework for Site 1237 that is in agreement with the biostratigraphic zonation of Sanfilippo and Nigrini (1998) and Moore (1995) and the shipboard magnetostratigraphy using the age assignments of Cande and Kent (1995). According to the Geomagnetic Polarity Timescale, the ages of 21 radiolarian datums are defined, covering the time interval of the last 11.5 m.y.

## STRATIGRAPHY

The purpose of this chapter is to point the readers to the publications that significantly complement shipboard biostratigraphic information contained in the Leg 202 *Initial Reports* volume (Mix, Tiedemann, Blum, et al., 2003) rather than discussing the details of postcruise stratigraphic work.

Studies on calcareous nannofossil biostratigraphy (**Flores et al.**, this volume) and radiolarian stratigraphy (**Weber and Pisas**, this volume) enhanced the Miocene–Pleistocene zonation of Leg 202 sites. Stable isotope records in combination with orbitally tuned cyclostratigraphy refined the Pleistocene stratigraphy at Sites 1233 and 1234 (Lamy et al., 2004; Heusser et al., 2006a); the Miocene–Pliocene stratigraphy at Sites 1236, 1237, 1239, and 1241 (**Tiedemann et al.**, this volume; Holbourn et al., 2005); and the Oligocene stratigraphy around the late Oligocene climate optimum at Site 1237 (**Flower and Chishom**, this volume).

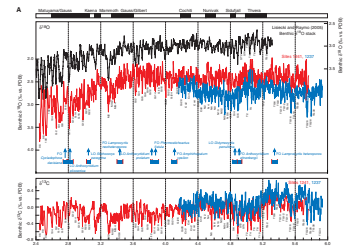
The stratigraphies at Sites 1233 and 1237 deserve closer attention, as they rank among the best hemipelagic and pelagic reference sections from the South Pacific. Site 1237 provided a complete pelagic Oligocene (~31 Ma) to Holocene sediment sequence that was relatively unmodified by burial diagenesis and was fully recovered using the advanced piston corer (APC). Good preservation of calcareous microfossils to the base of the Oligocene, the late Miocene–Holocene presence of siliceous microfossils, and a nearly complete magnetostratigraphy provided an excellent basis for postcruise stratigraphic refinements. Although the completion of a high-resolution upper Paleogene and Neogene stratigraphy at Site 1237 will take several more years, substantial progress has been made within particular time intervals. The work of **Flores et al.** (this volume) significantly improves the Pleistocene calcareous nannofossil biostratigraphy by confining 11 events of key biostratigraphic marker species using a sampling resolution of 10–30 cm for the last 0.5 m.y. and 75–150 cm for the time interval from 0.5 to 2.0 Ma. **Weber and Pisas** (this volume) present a first radiolarian biostratigraphic framework for the time interval of the last 11.5 m.y. that is consistent with the biostratigraphic zonation of Sanfilippo and Nigrini (1998) and Moore (1995). The ages for key radiolarian datums are derived from shipboard magnetostratigraphy using the age assignments of Cande and Kent (1995).

The goal to establish a complete stable isotope chronostratigraphy for Site 1237 represents a joint effort of various groups and has not yet been completed. So far, high-resolution benthic stable isotope records

in combination with orbitally tuned cyclostratigraphy provide detailed age control for the time intervals from 2.0 to 6.0 Ma (Tiedemann et al., this volume) and 12.7 to 14.7 Ma (Holbourn et al., 2005), although sedimentation rates were relatively low (1–3 cm/k.y.). Flower and Chisholm, this volume) established a benthic isotope record for the time interval from 25.2 to 27.3 Ma.

Figure F4A provides an example of integrating bio-, magneto-, and isotope stratigraphy on the basis of an orbitally tuned timescale for the time interval 2–6 Ma. Tiedemann et al. (this volume) generated an orbitally tuned timescale by correlating the high-frequency variations (precession- and obliquity-related cycles) in GRA density and benthic  $\delta^{13}\text{C}$  and  $\delta^{18}\text{O}$  to the orbital solution of Laskar et al. (1993). The orbitally derived ages of Pliocene magnetic reversal boundaries between the base of the Réunion and the top of the Thvera coincide with those of the ATNTS2004 timescale (Lourens et al., 2004), except for the top of Kaena and the base of Sidufjall. At Site 1237, the astronomical age for the top of Kaena is about one obliquity cycle older. The base of Sidufjall appears to be about one precession cycle younger. The astronomically tuned isotope stratigraphy is in agreement with that from Atlantic Site 925/926 (Tiedemann and Franz, 1997; Shackleton and Hall, 1997) but deviates from the orbitally tuned LR04 benthic  $\delta^{18}\text{O}$  stack (0–5.3 Ma) (Lisiecki and Raymo, 2005) prior to MIS Si6 (4.9 Ma). The isotope nomenclature from MIS 96 to Si6, the stage identification and age assignments of recognized oxygen isotope stages are almost identical between the LR04 benthic  $\delta^{18}\text{O}$  stack and the Leg 202  $\delta^{18}\text{O}$  records from 2.4 to 4.9 Ma. However, the correlation of identical isotope stages is ambiguous in the time interval from 4.9 to 5.3 Ma, which comprises the Thvera Chron, although the age models of Tiedemann et al. (this volume) and Lisiecki and Raymo (2005) provide nearly identical ages for the top and base of Thvera. Within this interval, the LR04  $\delta^{18}\text{O}$  stack represents an average of five aligned (globally distributed) benthic  $\delta^{18}\text{O}$  records, whereas three of them were aligned to an initially produced transitional high-quality stack created from Sites 846 and 999. The LR04  $\delta^{18}\text{O}$  stack identifies MIS T7 (~5.05 Ma) as the most pronounced  $\delta^{18}\text{O}$  minimum of the last 5.3 m.y (Fig. F4A). This minimum may correspond to MIS T5 or T3 at Sites 1237 and 1241, which are one or two obliquity cycle(s) younger, respectively. At Sites 1237 and 1241, the  $\delta^{18}\text{O}$  signal-to-noise ratio is relatively low between 4.8 and 5.3 Ma (except for MIS T5 and T3), and thus the benthic  $\delta^{18}\text{O}$  records are far from being an excellent tuning medium. Spectral analyses in the depth domain (Tiedemann et al., this volume) suggest that the Leg 202 records of benthic  $\delta^{13}\text{C}$ , GRA density, and sand content are better suited for orbital tuning. The benthic  $\delta^{13}\text{C}$  amplitudes provide a surprising clarity of the 41-k.y. signal across this interval, in contrast to the  $\delta^{18}\text{O}$  records. In addition, the GRA density record from Site 1237 and the sand content record from Site 1241 provide significant variability at precession-related frequencies. Thus, Tiedemann et al. used a multi-proxy tuning approach (taking priority over  $\delta^{18}\text{O}$ ) to create the Leg 202 age model for this interval. This may explain the possible deviation between the LR04  $\delta^{18}\text{O}$  stack and the Leg 202 records, as the orbital tuning of the LR04  $\delta^{18}\text{O}$  stack is solely based on oxygen isotope variability. The deviation between the two age models becomes evident when comparing the  $\delta^{13}\text{C}$  records from Leg 202 (Sites 1237 and 1240) with the  $\delta^{13}\text{C}$  record from Site 846 (Fig. F4B), which was, in addition to that from Site 999, one of the two key records used to create the LR04  $\delta^{18}\text{O}$  stack. (As the  $\delta^{13}\text{C}$

F4. Integrating radiolarian-, magneto-, and isotope stratigraphy, p. 44.



record from Site 999 has no composite depth, it is not considered in Fig. F4B). Within the critical time interval from 5.3 to 4.6 Ma, all  $\delta^{13}\text{C}$  records are well correlated between  $\sim 4.9$  Ma (MIS ST1) and 4.6 Ma (MIS N8) and vary nearly in phase with orbital obliquity. Prior to  $\sim 4.9$  Ma, however, the  $\delta^{13}\text{C}$  record from Site 846 lacks correlation with both orbital obliquity and the Leg 202  $\delta^{13}\text{C}$  records. This argues for a possible mismatch between the LR04  $\delta^{18}\text{O}$  stack and the orbital record prior to 4.9 Ma.

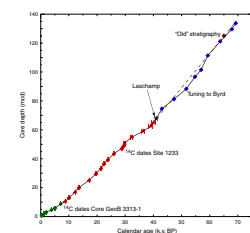
Holbourn et al. (2005) developed an orbitally tuned benthic isotope stratigraphy for the middle Miocene time interval (12.7–14.7 Ma) at Site 1237, which marked the Earth's final transition into an icehouse climate  $\sim 13.9$  m.y. ago. The new chronology was generated by initially matching the 400- and 100-k.y. amplitude variations in the  $\delta^{18}\text{O}$  series to the latest astronomical solution (Laskar et al., 2004) and then adjusting individual obliquity-scale cycles. The most surprising feature of the  $\delta^{18}\text{O}$  time series is the transition from high-amplitude obliquity-paced variations dominant between 14.7 and 13.9 Ma to eccentricity-paced fluctuations between 13.8 and 13.1 Ma. The timing of this change in  $\delta^{18}\text{O}$  frequency parallels the mid-Miocene expansion of the Antarctic ice sheet and is consistent with a change in the amplitudes of orbital obliquity and eccentricity. Flower and Chishom (this volume) generated a benthic stable isotope record for the late Oligocene time interval from 25.2 to 27.3 Ma and tied the onset of the late Oligocene climate optimum to GTS 2004 (Gradstein et al., 2004) by using isotope data and shipboard magnetostratigraphy. Their results suggest an age of 26.35 Ma for the final decrease in  $\delta^{18}\text{O}$ , marking the initiation of the late Oligocene climate optimum. This climatic shift is closely associated with the LO of the planktonic foraminifer *P. opima*. These studies demonstrate the potential for completing a high-resolution, orbitally tuned stable isotope chronostratigraphy for the upper Cenozoic and Neogene that in addition includes a tight framework of bio- and magnetostratigraphy at a single site.

Although the 135.7-mcd composite sequence from Site 1233 only spans the time interval of the last 70 k.y., it comprises a time resolution that allows centennial-scale reconstructions of climate variability. This in combination with an excellent and unprecedented high-resolution magnetostratigraphy makes it an outstanding stratigraphic reference section for the South Pacific (Lund et al., this volume a). Comparison of detailed rock magnetic and paleomagnetic records from three different holes at Site 1233 clearly demonstrate reproducible, pervasive, and distinctive centennial- ( $\sim 150$ – $300$  yr) and millennial-scale environmental, climatic, and geomagnetic field variability (Lund et al., this volume b). In addition, more than 20 AMS  $^{14}\text{C}$  age datings led to a detailed age model (Fig. F5) (Lamy et al., 2004; Kaiser et al., 2005; Kaiser, 2005) that suggests extremely high sedimentation rates, ranging between  $\sim 1.4$  m/k.y. in the Holocene to an average of  $\sim 2.2$  m/k.y. during MIS 2–4.

## TECTONICS AND CLIMATE

One of the keys to understanding climate change on tectonic time-scales is the detailed knowledge of changes in oceanic and atmospheric circulation triggered by tectonic processes such as the opening and closing of oceanic gateways and the uplift history of great mountain belts. The upper Paleogene and Neogene sequences from Leg 202 (Sites 1236–1242) form a latitudinal transect off the coast of Central and South

F5. Age model of the composite sequence at Site 1233, p. 47.





In comparison, recently reported SST reconstructions from Pacific Sites 846 (Lawrence et al., 2006) and 847 (Wara et al., 2005), which are positioned farther south of Site 1241 in the eastern equatorial upwelling region, also reveal significant Pliocene long-term cooling (Fig. F8). However, the timing for the onset of the cooling deviates significantly, even though both sites are located in the equatorial cold tongue within the influence of the South Equatorial Current (SEC). The SST record from Site 847 (estimated from Mg/Ca measurements in *G. sacculifer*) suggests that equatorial cooling began at ~2.5 Ma, whereas the alkenone-based SST record from Site 846 suggests that the cooling started at ~4.3 Ma, well before the intensification of NHG. This difference in timing between sites cannot be ascribed to paleodrift, as both sites drifted eastward toward the center of the cold tongue (if at all, this probably only predated the true regional cooling at the two sites). The different timing of the Pliocene cooling in the equatorial east Pacific (EEP) most likely resulted from a combination of global long-term cooling, regional changes in surface water conditions, and/or from differences in the depth habitat between species responsible for the SST proxy measured (as the alkenone unsaturation index of the organic remains from coccolithophorids should reflect shallower water temperatures than those derived from the Mg/Ca ratio of the mixed-layer dweller *G. sacculifer*). Hence, the present evidence makes it difficult to define a simple mechanism for Pliocene EEP cooling and to evaluate to which degree the cooling contributed to or resulted from NHG. However, the gradual and long-term character of Pliocene climate change points to slow tectonic forcing such as the closing of gateways or mountain uplift. Cane and Molnar (2001) proposed that the restriction of the Indonesian Gateway between 4 and 3 Ma probably reduced the atmospheric heat transport from the tropics to the higher northern latitudes, thereby cooling the arctic regions. The shoaling of the CAS may have increased the moisture supply to high northern latitudes via an intensification of the Atlantic meridional overturning circulation (Driscoll and Haug, 1998). Enhanced freshwater delivery to the Arctic Ocean via Siberian rivers could facilitate sea ice formation, thereby increasing the albedo and reducing the heat transfer from the ocean into the atmosphere. Mountain uplift (Tibetan Plateau and Andes) may have led to weathering-induced CO<sub>2</sub> removal and to changes in southeast Pacific atmospheric circulation during the Miocene and Pliocene (Raymo and Ruddiman, 1992; Hay 1996). Although the precise timing of when these tectonic processes became climatologically efficient is not well constrained, they have to be considered as an indirect cause of NHG and tropical cooling in the east Pacific.

Although the link between tropical gateway closures and NHG is still a matter of debate (Berger and Wefer, 1996; Haug and Tiedemann, 1998; Cane and Molnar, 2001; Ravelo et al., 2004; Haug et al., 2005), paleoceanographic studies suggest a close link between the formation of the Panama Isthmus and major oceanographic changes during the early Pliocene between 4.7 and 4.2 Ma, when shoaling of the CAS reached a critical threshold for upper ocean water mass exchange (Keigwin, 1982; Haug et al., 2001; **Steph et al.**, 2006, this volume; **Groeneweld et al.**, this volume). Restricted exchange of Pacific-Caribbean surface water masses led to the establishment of the modern Atlantic/Pacific salinity contrast that may be linked to the atmospheric net freshwater transport from the tropical Atlantic and Caribbean into the EEP (e.g., Jousaume et al., 1986; Benway and Mix, 2004). In addition, results from general circulation models as well as paleoceanographic

studies suggest reorganization of equatorial Pacific surface circulation and an increased volume transport of heat and salt into the North Atlantic via an intensified Gulf Stream, favoring North Atlantic Deep Water (NADW) formation and Atlantic carbonate preservation (Maier-Reimer et al., 1990; Farrell et al., 1995; Tiedemann and Franz, 1997; Cannariato and Ravelo, 1997; Mikolajewicz and Crowley, 1997; Haug and Tiedemann, 1998; Billups et al., 1999; Haug et al., 2001; Prange and Schulz, 2004).

Site 1241 was drilled in an ideal position to monitor oceanographic changes that may have resulted from the closure of the CAS, as it is close to the gateway region and comprises a complete late Neogene sequence of carbonate-rich and well-preserved foraminifers (except during the late Miocene carbonate crash noted by Lyle et al., 1995) from relatively shallow water depth (2000 m). Steph et al. (this volume) assessed changes in upper ocean stratification by comparing Mg/Ca temperature and  $\delta^{18}\text{O}$  records from shallow- and deep-dwelling planktonic foraminifers (*G. sacculifer* and *G. tumida*) that span the time interval from 5.5 to 2.5 Ma at Site 1241. Their study indicates an early Pliocene shoaling of the tropical east Pacific thermocline that was marked by a 6°C temperature decrease (5.3–4.0 Ma) at the bottom of the photic zone, associated with two major steps at 5.3 and 4.5 Ma (Fig. F8). This decrease cannot be explained by the site's tectonic drift (Fig. F8). Instead, the early Pliocene shoaling seems to be a regional phenomenon of the tropical northeast Pacific, expanding to Sites 847 and 851, which are located ~1000 and 2000 nmi southwest of Site 1241, respectively. At Sites 847 and 851, planktonic  $\delta^{18}\text{O}$  records from *G. tumida* document an increase in  $\delta^{18}\text{O}$  after ~4.5 Ma (Cannariato and Ravelo, 1997; Chaisson and Ravelo, 2000; Wara et al., 2005; Ravelo et al., 2006), which has been interpreted as a temperature decrease at the bottom of the photic zone by assuming that the  $\delta^{18}\text{O}$  records primarily represent a temperature signal.

The timing of the thermocline rise suggests a causal relationship to the shoaling of the CAS, as suggested by modeling experiments with the UVic Earth System climate model (Steph, 2005; Schneider and Schmittner, 2006). Model simulations for different sill depths suggest subsurface cooling of ~3°C and thermocline shoaling at Site 1241 when the sill depth rose from 700 to 130 m, as well as freshening in the tropical Pacific mixed layer when the sill depth rose to <130 m. Accordingly, thermocline shoaling may have occurred prior to freshening. The study of Groeneveld et al. (this volume) suggests significant freshening at Site 1241 after 3.7 Ma. The general consent between model results and proxy data corroborates a link to the progressive closure of the CAS rather than linking the observed changes to a response that may have resulted from the Pliocene constriction of the Indonesian Gateway (Cane and Molnar, 2001) or from the uplift of the Andes.

The Neogene uplift of the Andes Mountains is likely to have caused extensive changes in South American climate, wind-driven oceanic surface circulation, and biogenic productivity by reorganizing the pattern of atmospheric circulation and the hydrological cycle. Sedimentological and paleobotanical evidence from the Atlantic and the Pacific sides of the Andes as well as the frequent occurrence of ash layers in Leg 202 sediment records point to major uplift phases since ~12 Ma that were associated with intense volcanism and aridification of the Atacama Desert (for details see Mix, Tiedemann, Blum, et al., 2003). Paleobotanical evidence as summarized by Gregory-Wodzicki (2000) suggests a different uplift history for the central and northern Andes. These data

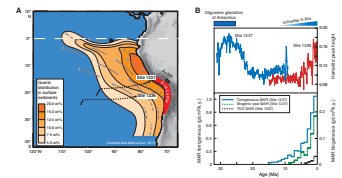
suggest that the central Andes had attained no more than half of modern elevation by ~10 Ma and imply surface uplift of ~2000–3500 m since the late Miocene. Major uplift of the Colombian Andes has been suggested to occur at a later stage, between 2 and 5 Ma, reaching no more than 40% of modern elevation by ~4 Ma and modern height by ~2.7 Ma. Based on oxygen isotopes in lacustrine carbonates, Garziona et al. (2006) infer rapid rise of the Bolivian Altiplano to its current elevation between ~10.3 and ~6.8 Ma (with a data gap from 10.3 to 7.6 Ma), coincident with an abrupt increase in physically weathered chlorite and oxide mineral evidence for increasing terrigenous aridity from 8 to 7 Ma recorded in marine sediments off the Amazon (Harris and Mix, 2002) and with sedimentological data from Atacama Desert that indicate that desertification commenced at ~8 Ma (Hartley and Chong, 2002).

Uplift-induced paleoceanographic changes in the eastern South Pacific are expected to derive mainly from reorganizations in atmospheric circulation. Progressive uplift of the Andes formed a barrier for the trade winds, which forced the low-level high-velocity winds on the western side to follow the coastline (Hay, 1996). The associated increase in trade wind strength should have initiated a chain reaction of environmental changes, including enhanced coastal upwelling, lower SSTs, reduced evaporation, and increased onshore aridity (desertification of the Atacama). South Pacific Sites 1236 and 1237 are best suited to prove such hypothesized climatic and oceanic changes as well as possible thresholds and feedbacks that might emerge from the uplift of the Andes.

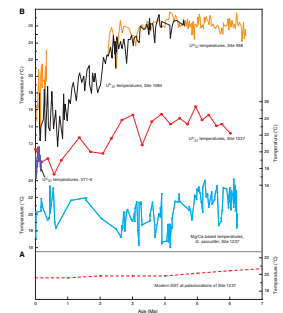
At both Sites 1236 and 1237, eolian iron oxides are accompanied by a significant eolian siliciclastic fraction since the late Miocene (Fig. F9). After ~8 Ma, increases are evident in both hematite content at Site 1236 (especially after ~6 Ma) and total dust flux at Site 1237, indicating enhanced eolian deposition likely sourced from the Atacama Desert. Moreover, the increases in eolian deposition and aridification are paralleled by a pronounced increase in productivity at Site 1237 (Fig. F9).

To characterize late Neogene variations in the thermal structure of the upper water column at Site 1237, Abe et al. (this volume) and Wara and Ravelo (this volume) reconstructed alkenone- and Mg/Ca-derived SST records that span the time interval of the last 6 m.y. (Fig. F10). Assuming no changes in regional oceanography, tectonic drift of the site would predict long-term cooling of surface waters and shoaling of the thermocline (Fig. F10) over the past 6 m.y. as the site approached the coastal upwelling area off Chile. In contrast, the alkenone-derived SST record (Abe et al., this volume) suggests no marked trend and relatively warm temperatures between 5 and 3 Ma. However, temperatures significantly declined by more than 5°C since 3 Ma, a trend that was possibly amplified by the site's paleodrift. This cooling trend is consistent with that observed in other subtropical upwelling areas (e.g., Marlow et al., 2000) (Fig. F10), and the range of late Pleistocene temperature variability agrees with alkenone temperatures reconstructed at a nearby piston core (Calvo et al., 2001; Prahl et al., 2006). The alkenone-derived Pliocene–Pleistocene cooling trend, however, conflicts with Mg/Ca temperature reconstructions of Wara and Ravelo (this volume), which suggest no significant long-term temperature changes over the past ~6 m.y. at Site 1237 (the conversion of Mg/Ca ratios determined at tests from *G. sacculifer* was carried out by applying the equation of Anand et al., 2003) (Fig. F10). Another peculiarity is that the Mg/Ca-based mixed-layer temperatures are at times warmer than the alkenone-based surface temperatures, which is not very likely. Whether the absolute temperature estimates are biased by factors other than in situ temperature,

F9. Quartz in surface sediments of subtropical southeast Pacific, p. 51.



F10. Site 1237 annual-average SSTs and planktonic Mg/Ca temperature reconstructions, p. 52.



which affected the alkenone unsaturation index ( $U^{k_{37}}$ ), or the amount of  $Mg^{2+}$  incorporated into foraminiferal tests during calcification, which include, for example, diagenetic processes, selection of paleotemperature equations, and redistribution of sediment material, is difficult to assess without further data. The application of species-specific Mg/Ca temperature equations for *G. sacculifer* (Nürnberg et al., 2000; Dekens et al., 2002) instead of the multispecies equation of Anand et al. (2003) would have resulted in even warmer ( $\sim 1^{\circ}$ – $2^{\circ}$ C) mixed-layer temperatures (e.g., Steph et al., this volume). Effects such as preferential removal of  $Mg^{2+}$  in response to enhanced carbonate dissolution would result in lower Mg/Ca temperature estimates (e.g., Dekens et al., 2002). Another question is to what extent the  $U^{k_{37}}$  signal is biased by seasonal cycles in coccolithophorid production, as the  $U^{k_{37}}$ -SST calibration is based on annual mean SSTs (Müller et al., 1998). If the Mg/Ca signal of *G. sacculifer* and the sedimentary  $U^{k_{37}}$  signal at Site 1237 both primarily reflect that of the warm season, the alkenone-derived temperatures (Fig. F10) might be too low. Assuming that the long-term trends in both temperature records are reliable, at least, provides an interesting perspective. The habitat-related temperature gradient between both temperature records may point to enhanced stratification prior to  $\sim 2.5$  Ma and to an enhancement in upwelling over the past 2.5 m.y., when subsurface and surface temperatures were more similar. This interpretation would be consistent with the observed increase in trade wind strength, continental aridification (Atacama), and productivity as indicated by a strengthened increase in dust, organic carbon, and biogenic opal accumulation rates (Fig. F9). The timing of these wind-induced changes between 3.0 and 2.5 Ma suggests amplification in atmospheric circulation that may have been driven as a threshold response to a steeper pole-equator temperature gradient, owing to the amplification of polar glaciation rather than to the uplift of the Andes.

This hypothesis is further constrained by paleoceanographic evidence from the Benguela upwelling system off the coast of southwest Africa. The Benguela upwelling system is analog to the eastern boundary current and upwelling system off western South America, but along a mountain range that experienced no significant uplift during the late Neogene. Marlow et al. (2000) presented an alkenone-derived SST record (0–7 Ma) from the Benguela upwelling system that is consistent with the general evolution of SSTs at Site 1237 (Abe et al., this volume). SSTs of the Benguela upwelling system remained warm and relatively uniform during the late Miocene and the early Pliocene and significantly declined by  $\sim 10^{\circ}$ C since 3.2 Ma (Fig. F10). The decrease in SST in the Benguela system has been interpreted to reflect enhanced wind-driven upwelling, consistent with increased trade wind strength and aridification of Africa throughout the cooling transition (amplification of NHG), as evidenced by records of eolian dust flux to marine sediments (Tiedemann et al., 1994; Ruddiman and Janecek, 1989; Hovan and Rea, 1991). The similarity of temporal changes in SST, upwelling, and dust flux between the Benguela and Chile upwelling systems suggests that the uplift of the Andes was probably of secondary importance for generating the observed oceanic changes at Site 1237 during the last 6 m.y., as the Benguela upwelling system was not affected by mountain uplift. Hence, the expected atmosphere-oceanic response of the southeast Pacific to the uplift of the Andes, if any, likely occurred prior to 6 Ma during the time of major uplift. A full test of this hypothesis must await additional reconstructions of temperature and other oceano-

graphic properties in the interval that spans the likely time of Altiplano uplift near 8 Ma.

## ORBITAL-SCALE CLIMATE VARIABILITY

The Milankovitch orbital hypothesis on the climate effects of orbital precession, obliquity, and eccentricity is now generally accepted as a primary pacing mechanism for late Pleistocene ice ages (e.g., Imbrie et al., 1989, 1992, 1993). Based on this finding, tuning of climate records to orbital variations provides a primary tool for chronology development over late Cenozoic time (e.g., Shackleton et al., 1995b). In an application of this method, Tiedemann et al. (this volume) developed internally consistent orbitally tuned timescales for the interval 6–2.5 Ma from four Leg 202 sites (1236, 1237, 1239, and 1241), providing an exceptional framework for further studies of regional climate change.

In spite of widespread agreement on the importance of Earth's orbit to climate change, the mechanisms that translate orbital changes in the global and regional climate changes remain under debate (e.g., Maasch and Salzman, 1990; Muller and MacDonald, 1997; Shackleton, 2000). In particular, it is not clear to what extent climate varies internally in a set of natural oscillations, or if on long timescales it responds directly to external forcing, or if it rapidly switches between discrete modes, given either random or systematic forcing. One likely path to illuminate such mechanisms is to examine the evolution of the orbital climate cycles as the sensitivity of response, relative to orbital forcing, rises and falls through time (Pisias et al., 1990).

A particular puzzle is the 100-k.y. climate cycle, which arose most recently in mid-Pleistocene time, ~1 m.y. ago (Pisias and Moore, 1981). The primary signature of this so-called Middle Pleistocene Transition (MPT) is a frequency change in global ice volume oscillations from a dominant 41-k.y. cycle to a 100-k.y. cycle recorded in benthic foraminiferal  $\delta^{18}\text{O}$ . This change in the frequency of primary climate rhythms occurred in the absence of any significant changes in the pattern or amplitude of orbital forcing and thus required a fundamental change in processes internal to the Earth system. Most hypotheses for the MPT invoke a threshold response to a gradual long-term cooling, which is often attributed to an assumed secular decrease in atmospheric  $\text{pCO}_2$  (e.g., Raymo, 1997; Raymo et al., 1997; Mudelsee and Schulz, 1997; Paillard, 1998; Berger et al., 1999; Lea, 2004; Lisiecki and Raymo, 2005). Further rhythmic variations in  $\text{CO}_2$  provide a likely feedback mechanism for sustaining the 100-k.y. climate cycle as a response to greenhouse feedbacks (Pisias and Shackleton, 1984; Shackleton, 2000; EPICA Community Members, 2004).

McClymont and Rosell Melé (2005) demonstrated that the MPT was not simply a development within the Northern Hemisphere ice sheets and high-latitude climates but was preceded by a significant change in the tropical Pacific circulation system, thereby identifying the tropics as a potential driver of the MPT. They proposed that the development of the modern zonal temperature gradient in the equatorial Pacific (1.2–0.9 Ma) intensified Walker circulation and reduced heat flux but increased moisture transport to high latitudes, leading to the development of more extensive ice sheet growth and the shift toward the 100-k.y. world.

Other ideas for long-term change in the sensitivity to orbital forcing include mountain uplift (Ruddiman and Raymo, 1988) or erosion of to-

pography and rise of plateaus (Berger and Jansen, 1994) that allowed larger glaciers to survive through smaller cycles of orbital precession (dominated by 23- and 19-k.y. cycles), eventually creating a 100-k.y. climate cycle (although this would also likely yield a 412-k.y. cycle, which is not observed) (Imbrie and Imbrie, 1980). Gildor and Tziperman (2001) also note long-term cooling of the deep sea at polar outcrops, which influenced sea ice distributions. Ruddiman (2006) suggests that the abrupt rise of the 100-k.y. cycle at the MPT results from greenhouse feedback and the interaction of forcing from the 23- and 41-k.y. orbital cycles (but note that nonlinear interaction of these two cycles yields sum and difference tones of 14 and 52 k.y., so additional mechanisms are still needed).

Clark and Pollard (1998) and Clark et al. (in press) propose an alternate mechanism for the origin of the 100-k.y. climate cycle, in which gradual erosional exposure of crystalline Precambrian Shield bedrock yielded a high-friction substrate that supported thicker ice sheets, with an attendant change in their response time to orbital forcing. In this scenario, 100-k.y. cycles arise as a natural consequence of the dynamics of thick and extensive ice sheets.

A puzzle in this regard, however, is that 100-k.y. cycles have been noted in various components of the Earth system at times prior to the MPT (e.g., Mix, 1987; Mix et al., 1995a; [Groeneveld et al.](#), this volume, [Steph et al.](#), this volume; Holbourn et al., 2005). Do these earlier 100-k.y. climate cycles arise from mechanisms similar to the Pleistocene cycles, or are they fundamentally different? Do they provide precursor “templates” in the climate system, which could then be entrained through feedback mechanisms to grow a Pleistocene 100-k.y. ice sheet cycle in a gradually cooling climate? Or are these other examples simply independent and unrelated features of the climate system?

Sites from Leg 202 that provide new opportunities for study of the long-term evolution of orbital-scale climate variability include Sites 1236 and 1237 in the subtropical South Pacific (both exceptionally long sequences sampled with the APC), Sites 1238–1240 in the eastern equatorial Pacific cold tongue (EEPCT), and Sites 1241 and 1242 in the eastern tropical north Pacific warm pool of the Panama Bight. At this stage of Leg 202 studies, orbital-scale records of upper ocean and deep-sea variability have focused on the time interval 2.5–5.0 Ma, including the so-called early Pliocene “golden age” of global warmth (Sarnthein and Fenner, 1988) that was characterized by relatively small polar ice sheets and warmer deep-sea temperatures (Sarnthein and Tiedemann, 1989; Shackleton et al., 1995b; Mix et al., 1995b), as well as the early stages of cooling toward the Pliocene–Pleistocene ice ages of the past ~2.5 m.y. (Fig. F6). This is a time generally found to be dominated by 41-k.y. climate cycles. In addition, other Leg 202 studies focus on the interval from 12.7 to 14.7 Ma, an analogous time of cooling following the so-called Miocene climatic optimum (Fig. F6).

[Groeneveld et al.](#) (this volume) combined Mg/Ca paleotemperature estimates with  $\delta^{18}\text{O}$  measurements of the near-surface dwelling foraminifer *G. sacculifer* over the interval 4.8–2.4 Ma at Site 1241 in order to assess the sensitivity of orbital-scale climate variability in the eastern Pacific warm pool (EPWP) to Pliocene global warmth, closure of the Panama Isthmus, and global cooling during early development of the Pliocene–Pleistocene ice ages from ~3.7 to 2.4 Ma (Fig. F8). The beginning of this interval is noted by the development of a strong and shallow thermocline from ~4.8 to 4.0 Ma and to an increasing gradient of  $\delta^{13}\text{C}$  from the intermediate waters (at Site 1236) to the thermocline

(*Neogloboquadrina dutertrei* at Site 1241) developing strongly after 3.3 Ma. This likely reflects a change in the high-latitude source waters that feed the Equatorial Undercurrent (EUC) in response to polar cooling and the intensification of NHG (Steph et al., this volume). The shallowing thermocline has little or no apparent effect on SST (Steph et al., this volume; Groeneveld et al., this volume).

During the early Pliocene time interval of 4.8–3.7 Ma, benthic foraminiferal  $\delta^{18}\text{O}$  is dominated by the well-known 41-k.y. (obliquity) cycle with minor contributions from the 23-k.y. (precession) effect. In contrast, Mg/Ca surface temperatures at Site 1241 are dominated by the 23-k.y. precession cycle, along with a ~100-k.y. cycle that is associated either with orbital eccentricity or a nonlinear response to precession (Groeneveld et al., this volume). The  $\delta^{18}\text{O}$  of *G. sacculifer* at Site 1241 also includes strong variability in the precession and eccentricity bands, as does the calculated paleosalinity record, which is consistent with ideas of tropical origins of such cycles related to insolation and monsoon interactions with the continents (Crowley et al., 1992).

During the later interval of 3.7–2.4 Ma, Groeneveld et al. (this volume) find that benthic  $\delta^{18}\text{O}$  (presumed to reflect mostly ice volume) and planktonic formaminiferal Mg/Ca paleotemperatures at Site 1241 are both dominated by ~41-k.y. cycles, reflecting the growing influence of high-latitude processes on tropical climates. The  $\delta^{18}\text{O}$  of *G. sacculifer* and estimates of ice volume–corrected paleosalinity contain more long-period variability near the 100-k.y. cycle, however, suggesting continued variations in the tropical hydrologic cycle related to precession and eccentricity. Such a result is consistent with the finding of Mix et al. (1995a) of a persistent ~100-k.y. cycle in biogenic sedimentation at Site 846. At that site, the phase of the 100-k.y. cycle of sedimentation is synchronous with orbital eccentricity prior to the MPT (suggesting local or regional responses to insolation as suggested by Crowley et al., 1992). After the transition, however, the phase of the 100-k.y. cycle of sedimentation shifts and synchronizes with orbit-lagging ice volume and polar temperatures (benthic  $\delta^{18}\text{O}$ ).

The observed dominance of precession-paced SST variations in the EPWP prior to ~3.7 Ma (Groeneveld et al., this volume), however, contrasts the cyclic temperature variability in the EEPCT as suggested by a recently published alkenone-based paleotemperature record from Site 846 (Lawrence et al., 2006). The authors emphasize a dominant 41-k.y. cycle of SST variability throughout the past 5 m.y. at Site 846 and an in-phase relationship with benthic  $\delta^{18}\text{O}$  wherever the obliquity-related signals are coherent. These alkenone temperature estimates from the SEC imply a tight coupling between SST variability in the equatorial Pacific cold tongue and high-latitude-driven climate processes associated with changes in global ice volume. In contrast, SST variability at Site 1241 in the EPWP prior to ~3.7 Ma, based on the Mg/Ca proxy, suggests a dominant response to low-latitude changes in seasonal insolation (and associated processes) associated with variations in precession. The threshold of the EPWP for a significant response to high-latitude obliquity forcing was probably low during the early Pliocene, when the volume of polar ice sheets and their variability were relatively small (Philander and Fedorov, 2003).

A number of mechanisms may explain the difference in cyclic SST variability between Sites 1241 and 846, including different dynamics in surface and subsurface currents, thermocline depth, wind field, and associated atmosphere-ocean couplings. Today, Site 1241 (~6°N) is posi-

tioned within the Intertropical Convergence Zone (ITCZ) region and reflects changes in surface water signatures of the NECC, which carries the return flow of relatively warm, low-salinity surface waters eastward out of the west Pacific warm pool. Site 846 (3°S) is positioned south of the ITCZ in the EEPCT, whereas SST depends on wind-driven (southeast trades) changes in upwelling and cold-water advection from the Humboldt Current. Lawrence et al. (2006) favor obliquity-driven changes in atmospheric CO<sub>2</sub> concentrations rather than vertical movements of the thermocline as a possible mechanism to explain SST variations at Site 846. If so, the obliquity-related temperature variability at Sites 846 and 1241 should provide similar phasing and amplitudes, which is testable by cross-spectral analyses. As variations in atmospheric CO<sub>2</sub> would synchronize tropical SST changes, other mechanisms must be responsible for the different dominance in cyclic SST variability between EPWP and EEPCT. One possible explanation relates to the different origin of surface water masses. Site 856 is directly influenced by the SEC, which sources Southern Ocean water masses. Site 1241 is influenced by surface water masses, which originate from the western Pacific warm pool. Modeling studies indicate that the western Pacific warm pool is not particularly sensitive to cooling of the EEPCT (e.g., Lee and Poulsen, 2005, 2006), mainly because of equatorial insolation. Therefore, the warm pool may serve as a buffer preventing Southern Hemisphere signals from appearing in the Northern Hemisphere at Site 1241.

Steph et al. (this volume) examined whether the difference in cyclic SST variability could be explained by local changes in thermocline depth. They demonstrate that planktonic Mg/Ca temperature and δ<sup>18</sup>O of the deep-dwelling planktonic foraminifers are good indicators of changes in thermocline depth, as both records match each other. Given that the high-resolution δ<sup>18</sup>O records of *G. tumida* from Sites 1241 (warm pool), 851 (warm pool, west of Site 1241) (Cannariato and Ravelo, 1997), and 1239 (1°S, upwelling region off Ecuador) (Steph, 2005) are almost identical in absolute values and orbital-scale variability during the early Pliocene, it is not very likely that changes in thermocline depth led to the observed differences in cyclic SST between the cold tongue and the warm pool in the tropical east Pacific. In this context, however, it is important to note that changes in SST and thermocline depth are not necessarily coupled. On a long timescale, Steph et al. (this volume) document that the early Pliocene shoaling of the thermocline (at, e.g., Site 1241) has little or no apparent effect on SST. On a shorter (late Pleistocene) timescale, Benway et al. (2006) present similar findings for decoupling of pycnocline intensity and SSTs. At this stage of Leg 202 data analyses and assessment, a possible explanation for the apparent difference in early Pliocene cyclic SST variability between Sites 1241 and 846 is that the EPWP more likely responded to local insolation changes, whereas the EEPCT was more directly linked to high-latitude processes, wind-driven thermocline dynamics, or possibly atmospheric CO<sub>2</sub> variability. We expect that further information from the west Pacific warm pool and the eastern boundary current and upwelling system off South America will help to assess whether these differences reflect true regional differences in climate response.

Steph et al. (2006) compare the planktonic foraminiferal δ<sup>18</sup>O and Mg/Ca records from Pacific Site 1241 with Caribbean Site 1000 and note the development of strong 23-k.y. cycles in the Caribbean related to orbital precession, in the interval 4.4–3.0 Ma, as the two oceans start to become isolated by the rise of the Central American Isthmus. These

authors argue that precessional forcing of El Niño events, as predicted for the late Pleistocene by Clement et al. (1999), may have modulated flows of water between the Pacific and Atlantic, leading to a strong surface-ocean signal on the Caribbean side of the isthmus. Full closure of this isthmus eliminated the sensitivity to this effect. In the latest Pleistocene, Benway et al. (2006) examine the sensitivity of surface-ocean salinity to change at Site 1242, and although they find substantial millennial-scale changes, they find no significant changes from glacial to interglacial time, supporting the idea that the presence of an restricted but open CAS can change the sensitivity of low-latitude systems to orbital-scale changes.

Holbourn et al. (2005) examine the record of climate further back in time, during the middle Miocene global cooling event (14.7–12.7 Ma) (Fig. F6), to examine global climate changes in the orbital bands, pairing a new record from Site 1237 with a similar record from Site 1146. Both records were continuously cored and provide unprecedented resolution of the evolution in orbital-scale climate changes, with stable isotopes analyzed at 4- to 5-k.y. intervals and XRF scanned at ~1-k.y. intervals throughout the sequence. An orbitally tuned age model assumes that  $\delta^{18}\text{O}$  varies in phase with both orbital precession and obliquity, based on the orbital solution of Laskar et al. (2004). Within this interval, a rapid increase in benthic foraminiferal  $\delta^{18}\text{O}$  from 13.91 to 13.84 Ma records an increase in continental ice volume (constrained also by benthic foraminiferal Mg/Ca paleotemperature estimates at other sites [Lear et al., 2000]). Associated with the growth of continental ice sheets, a striking transition from a high-amplitude cycle in the 41-k.y. band to one in the 100-k.y. band occurred between 14.1 and 13.8 Ma. The strong 100-k.y. cycle in  $\delta^{18}\text{O}$  is also recorded in the XRF record of iron at Site 1237, although it is not clear whether this is related to iron input, dilution by varying biogenic production, or carbonate dissolution cycles.

Although qualitatively similar to the better-known development of 100-k.y. climate cycles in the MPT, the Miocene 100-k.y. cycles are of lower amplitude and precede the development of the ice sheets by as much as a few 100 k.y., whereas the Pleistocene 100-k.y. cycles develop after a long interval of gradual cooling ice sheet expansion. Further, lowering of marine carbon isotope values indicates a rapid transfer of organic carbon to inorganic carbon in the ocean system during the MPT (Raymo et al., 1997; Clark et al., in press), just the opposite of the observed increase in  $\delta^{13}\text{C}$  across the mid-Miocene transition (Holbourn et al., 2005). In both the Pleistocene and Miocene transitions, a significant ~400-k.y. cycle is found in benthic  $\delta^{13}\text{C}$ , which may be related to eccentricity or precession control of the carbon cycle (Mix et al., 1995b; Holbourn et al., 2005). Under the assumption that a positive shift in  $\delta^{13}\text{C}$  implies increased burial of  $^{13}\text{C}$ -depleted organic matter, Holbourn et al. (2005) infer that the growing 100-k.y. climate cycles of the Miocene were “primed” by decreasing atmospheric  $p\text{CO}_2$  and triggered by increases in the amplitude of orbital eccentricity (noting that better proxies for past  $\text{CO}_2$  variability are sorely needed). Thus, the late Pleistocene 100-k.y. climate cycles are not unique in Earth’s history, and although the examples from the Miocene and Pleistocene are both associated with climate cooling, they occur under significantly different global boundary conditions, different global mean temperatures, and with different relationships to the carbon cycle. This important study issues a challenge to climatologists to understand multiple origins of

100-k.y. climate cycles that are now well documented in the geologic record.

## **MILLENNIAL-SCALE CLIMATE VARIABILITY: POLAR OR TROPICAL CAUSES?**

Understanding the mechanisms and patterns of millennial-scale climate changes has until now lacked high-resolution and precisely dated marine records from the Southern Hemisphere, particularly from the Pacific sector. Therefore, one of the major goals of Leg 202 was to improve the knowledge of pattern and causes of millennial-scale climate variability in the southeast Pacific, with a particular focus on the last glacial–interglacial cycle.

Modeling studies have shown that the southeast Pacific may play a crucial role for the transmission of temperature anomalies from high southern latitudes to the tropical Pacific both through intermediate water masses (e.g., Gu and Philander, 1997; Schmittner et al., 2003) and perhaps also via the surface currents along western South America. The latter linkage between the eastern boundary current system and the equatorial Pacific seems to be important on longer glacial to interglacial scales (Feldberg and Mix, 2003; Pisias and Mix, 1997) and appears to be at least partly valid likewise on millennial scales (Lea et al., 2006).

Traditionally, it has been thought that millennial-scale changes during the last glacial interval are driven either by instabilities in the Northern Hemisphere ice sheets (MacAyeal, 1993) or feedback related to Atlantic thermohaline circulation (e.g., Rahmstorf, 2002), driven by anomalous input of meltwater into the North Atlantic (e.g., Clark et al., 2001, 2004). In spite of extensive efforts, however, attempts to track all the sources of meltwater and mechanisms for thermohaline oscillations remain controversial (Broecker, 2006). Other ideas for the origin of millennial-scale climate changes may involve rhythmic solar forcing (Bond et al., 2001, 1997) or internal resonant oscillations of the coupled ocean-atmosphere system (e.g., Alley et al., 2001; Ganopolski and Rahmstorf, 2002; Schulz et al., 2002).

Millennial-scale climatic oscillations, in particular during MIS 3, have been detected in many places around the globe (e.g., recent compilations by Clark et al., 2001, and Voelker, 2002) and have been primarily explained by oceanic and atmospheric responses to North Atlantic climate change (Schmittner et al., 2003). However, other studies suggest an important role of both the tropics (including long-term properties of ENSO) and the Southern Ocean (Clement et al., 1999; Koutavas et al., 2002; Stott et al., 2002). For example, changes in SSTs in the tropical Pacific may have large impacts on the global hydrological cycle (Clement et al., 1999) and perhaps on greenhouse gases (Palmer and Pearson, 2003; Visser et al., 2003) and are thus of global significance. A model study of the last glacial climate, which includes calibration with SST estimates from Leg 202 and other studies (Hostetler et al., 2006), suggests that relatively small sea-surface warming in tropical and subtropical oceans can shift Northern Hemisphere ice sheets from positive to negative, meaning that the low-latitude oceans could trigger early phases of deglaciation or interstadial climate oscillations within the ice age. In addition, the high latitudes of the Southern Hemisphere (including sea ice around Antarctica) (Tziperman and Gildor, 2003) may provide controls of greenhouse gases and for resumption of Atlantic thermohaline

circulation after previous reductions (Knorr and Lohmann, 2003; Weaver et al., 2003).

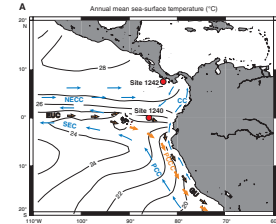
Several Leg 202 sites reveal sedimentation rates high enough to resolve millennial-scale or even centennial- to decadal-scale variations (Figs. F11, F12). These include the Chilean margin Sites 1233–1235 that contain very high sedimentation rate sequences (often >100 cm/k.y.) (Fig. F12) as well as two sites from the eastern tropical Pacific and the Panama Basin (Sites 1240 and 1242) (Fig. F11), where sedimentation rates are on the order of 10–20 cm/k.y. Taken together, these sites provide a unique paleoceanographic north-south transect to track millennial-scale variability from the northern margin of the Antarctic Circumpolar Current (ACC) (Site 1233) along the Humboldt Current northward (Sites 1234 and 1235) toward the tropics (Sites 1240 and 1242).

The initial published studies on millennial-scale climate variability based on Leg 202 focus on the southernmost Site 1233 located on the Chilean continental margin at ~41°S (Heusser et al., 2006b; Kaiser et al., in press, 2005; Lamy et al., 2004; Pisias et al., 2006) because the ~70-k.y.-old sequence recovered continuously with the APC extends over ~135 mcd, resulting in unprecedented high sedimentation rates, at least for the South Pacific (Fig. F5). In addition, the site is well located to compare both surface and deep ocean millennial-scale patterns to high southern latitudes. Today, SST gradients within the northernmost ACC are very large and intimately linked to the northern margin of the westerly wind belt, making this region very sensitive to latitudinal shifts of atmospheric and oceanographic circulation associated with the southern westerly winds. Site 1233 is located close to the southern Chilean coast (~40 km) and close to the northwestern margin of the PIS, which occupied a large area of southernmost South America during the last glacial. Thus, this unique location allows detailed comparison of various continental climate and paleoceanographic proxy records within the same archive and therefore avoids problems linked to age model uncertainties.

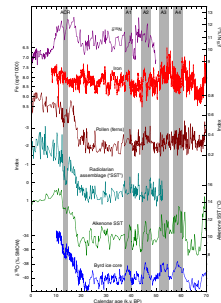
An important result from Site 1233 is the Antarctic timing and pattern shown in millennial-scale oscillations of alkenone-based SST (Lamy et al., 2004), as well as in radiolarian faunas and pollen assemblages (Pisias et al., 2006; Heusser et al., 2006b) that strongly support the concept of hemispheric asynchrony as seen in the ice records from Greenland and the Antarctic (Blunier and Brook, 2001; Lynch-Stieglitz, 2004) (Fig. F11). Other land-based records of glacier and vegetation changes from the Southern Hemisphere have not presented a clear picture, and some have been previously interpreted to support hemispheric synchrony with climate oscillations of Greenland, such as the Younger-Dryas climate interval (Denton et al., 1999; Lowell et al., 1995; Moreno et al., 2001). Many of these land-based studies have been performed in southern Chile directly onshore of Site 1233. Based on the high-resolution Fe content record from Site 1233 taken as a proxy record for glacial activity on land (Fig. F12), Lamy et al. (2004) suggested that part of these discrepancies might be due to a lagged response of PIS extent changes to SST changes offshore. Modeling studies show that southeast Pacific SSTs exert the dominant control on ice sheet extents in this region (Hulton et al., 2002). The Fe content record indeed shows a pattern that is very similar to that of the SST record, however with a lag of several hundred years.

Kaiser et al. (2005) extended the alkenone-derived SST record at Site 1233 back to 70 ka. They compared the Site 1233 record to the available SST records from the Southern Hemisphere mid-latitudes and conclude

F11. Millennial-scale sites and surface currents, p. 53.



F12. Comparison of proxy records, Site 1233 and Byrd ice core, p. 55.



that the Antarctic millennial SST pattern was probably a hemisphere-wide phenomenon. Furthermore, they performed SST gradient reconstructions over the complete latitudinal range of the Pacific eastern boundary current system. This reconstruction suggests strengthened and equatorward displaced subtropical gyre circulation during cold stages (MIS 2 and 4). Conversely, oceanic circulation was probably weakened, and the ACC, and associated westerly wind belt, moved southward during relatively warm periods (early MIS 3 and Holocene Climate Optimum).

For Termination 1, Lamy et al. (2004) further presented a paleosalinity record that supports these findings, as it shows a major meltwater input from the PIS ~1000 yr after initial deglacial warming. Kaiser et al. (in press) show that the close relationship of the Fe record and the SST pattern extends into the older part of the records (70–50 ka). During MIS 4, a delay of ~500 yr of PIS retreats relative to SST increases has been found, similar to that described for the coldest part of MIS 3 and 2 (Lamy et al., 2004). During early MIS 3 (~60–56 ka), synchronous variability in both records resembles the deglacial–Holocene time interval, reflecting either a meltwater pulse or a dominant control of Fe input by rainfall changes related to a rather small PIS.

At Site 1234 (1015 m water depth), the benthic foraminiferal stable isotope record clearly records changes in subsurface ocean temperature (and/or salinity) that are in phase with temperature changes in Antarctica (Mix et al., unpubl. data; Heusser et al., 2006a; Robinson et al., 2007; Blunier and Brook, 2001). Site 1234 is also particularly well suited for study of vegetation changes, as it is offshore the modern transition zone between the rainforest-dominated systems to the south and the Mediterranean (semiarid, summer dry) climate systems to the north. Pollen assemblages at Site 1234 reveal high-amplitude oscillations of rainforest vegetation, although lagging the benthic  $\delta^{18}\text{O}$  and Byrd ice core record by a few hundred years, suggesting either a ~1000-yr exponential response time that may reflect the time constant of vegetation response to regional climate change (Heusser et al., 2006a) or perhaps the influence of lagging ice sheets as noted by Lamy et al. (2004). However, some pollen assemblages from Site 1233 (Heusser et al., 2006b), interpreted as indicative of latitudinal shifts of the westerly wind belt, in general follow SST changes as reconstructed by radiolarian census data (Fig. F12). Pisias et al. (2006) performed statistical analyses suggesting that both the radiolarian and pollen data co-vary with Antarctic temperature, at least on timescales >3000 yr. They also confirm the systematic lag of changes in ice sheet extent based on the Fe content data (Kaiser et al., in press; Lamy et al., 2004).

Thus, the land-based studies that previously suggested linkage to Northern Hemisphere climate oscillations may be explained as Southern Hemisphere climate responses; however, some areas experienced a small local lag due to the response times of forest and ice systems. These studies highlight the importance of studying terrestrial proxies in the marine cores, thereby avoiding potential offsets induced by age model uncertainties.

These surface ocean data suggest a close coupling of the high southern latitudes and the tropical Pacific, which is consistent with the previous conclusions of Feldberg and Mix (2003) and Pisias and Mix (1997). Furthermore, Lea et al. (2006), based on a high-resolution Mg/Ca SST record from the Galapagos region, show that parts of the millennial-scale SST pattern of the eastern equatorial Pacific appear to be similar to the southern record from Site 1233. SST records currently being con-

structed at Site 1240 in the eastern tropical Pacific seem to confirm this finding (Cacho et al., 2006). The “Antarctic pattern” appears to be clearer in subsurface ocean records. Cacho et al. (2006) present preliminary data that suggest a clear Antarctic signal in an oxygen isotope record of a thermocline foraminifer species that primarily reflects variations within the EUC fed by Antarctic Intermediate Water (AAIW) (Fig. F11). These data support the concept of an “oceanic tunnel” mechanism for transmission of high-latitude climate changes to the tropical oceans (Liu and Yang, 2003), rather than solely by atmospheric forcing associated with greenhouse gases (Lea et al., 2006), at least on millennial scales.

Similarly,  $\delta^{15}\text{N}$  from Site 1234 suggests that denitrification in the southeast Pacific oxygen minimum zone follows an Antarctic climate pattern (Robinson et al., 2007; De Pol-Holz et al., 2006). Episodes of reduced denitrification recorded at Site 1234 represent times when more oxygen was present in the subsurface ocean. An increase in oxygen can be achieved through (1) lower temperatures, (2) higher ventilation rates, and/or (3) reduced oxygen demand in the low-latitude subsurface. Mechanisms that may account for the observations include changes in the chemical composition of SAMW, formed in the Subantarctic Zone of the Southern Ocean and ventilating the low-latitude thermocline (Robinson et al., 2007), or by local salinity control of Eastern South Pacific Intermediate Water (De Pol-Holz et al., 2006).

These preliminary data show that variability of Southern Ocean properties may play an important role in the transfer of climate signals in the Pacific realm during the last glacial. Sites 1233–1235 are particularly well located for assessing variations in the strength of AAIW through time (Fig. F3). Site 1235 monitors the boundary between the Gunther Undercurrent (GUC) (the poleward undercurrent, a relatively low oxygen water mass) and AAIW (a relatively high oxygen water mass). Site 1233 is located roughly in the core of AAIW and thus should provide the best available record of AAIW properties relatively close to its source in the Antarctic Subpolar Front. Finally, Site 1234 monitors the deeper boundary of AAIW in its zone of mixing with Pacific Central Water (PCW) (a relatively low oxygen water mass). Preliminary benthic and planktonic oxygen isotope records from Site 1233 show that changes in intermediate water properties closely track those of the surface water masses even on centennial to millennial timescales, albeit with a reduced amplitude (Ninnemann et al., 2006). These changes generally follow Antarctic timing as shown by alkenone SST records (Kaiser et al., 2005; Lamy et al., 2004). However, some of these changes, in particular during MIS 3, appear to be more abrupt in the ultra-high-resolution isotope records.

Sea-surface salinities in the EPWP off the west coast of Central America are closely coupled with excess precipitation relative to evaporation near the ITCZ (Benway and Mix, 2004). This region is noted for its extreme warmth (often  $>30^\circ\text{C}$ ), exceptionally low salinity (near 32), and a strong, shallow pycnocline (typically centered near 20–40 m depth). A portion of the net freshwater flux to the Panama Basin originates in the Atlantic or Caribbean (Jousaume et al., 1986), so low salinities here partially reflect the transport of freshwater from the Atlantic to Pacific Basins via the atmosphere. The dynamics of this transport are important because this relatively small transport of freshwater helps to maintain the relatively high salinity of the Atlantic Ocean—a key parameter in maintaining the global thermohaline “conveyor belt” circulation

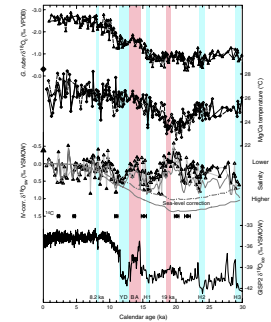
dominated by NADW production (Zaucker et al., 1994; Rahmstorf, 1995).

Indeed, millennial variations in paleosalinity with amplitudes as high as ~4 psu are documented at Site 1242 off Costa Rica, with a dominant period of ~3–5 k.y. during the glacial–deglacial interval and ~1.0–1.5 k.y. during the Holocene (Benway et al., 2006) (Fig. F13). Paleosalinity variations recorded at Site 1242 mimic Northern Hemisphere climate variability such as that in the Greenland ice core and North Atlantic (McManus et al., 2004). Similar Northern Hemisphere climate patterns have also been documented on the Pacific margin of Mexico (Ortiz et al., 2004) and North America (e.g., Behl and Kennett, 1996; Hendy et al., 2002; Mix et al., 1999).

In the EPWP, paleosalinity changes correspond to millennial-scale climate changes in the surface and deep Atlantic and the high northern latitudes, with generally higher (lower) paleosalinity during cold (warm) events (Fig. F13). The covariance of paleosalinity between the EPWP (Benway et al., 2006) and Caribbean (Schmidt et al., 2004) from the same latitudinal band suggests that ITCZ dynamics play a role in tropical hydrologic variability. There appears to be no significant change in paleosalinity of the EPWP in glacial relative to interglacial times, suggesting that changes in the tropical system do not respond passively to events of the high northern latitudes. Following the LGM, higher than average interbasin salinity contrast occurs during warmer intervals such as the Bølling/Allerød and early Holocene climatic optimum, and lower than average interbasin contrast corresponds to colder periods such as the Younger Dryas and Heinrich event H1, although the timing of abrupt changes is not identical to the high-latitude events. Phase calculations suggest the possibility of a lead of interbasin salinity contrast over Atlantic meridional overturning circulation by as much as ~1 k.y. The EPWP paleosalinity and interbasin contrast records are also coherent with Atlantic  $\delta^{13}\text{C}$  records (McManus et al., 1999, 2004; Oppo et al., 2003) at periods of 3–5 k.y. The lack of glacial–interglacial contrast in the hydrologic system and the possibility that tropical changes may lead high-latitude climate and circulation changes suggest that North Atlantic circulation is in part influenced by changes in westward vapor transport in the tropics, via control of the North Atlantic salinity budget and thermohaline overturn, as originally suggested by Weyl (1968).

Although much work on high-resolution climate changes continues, already the new materials recovered during Leg 202 have changed the view of the global distribution of millennial-scale climate change. It is now clear that millennial-scale climate and biogeochemical systems of the southeast Pacific and Chile are closely aligned with those recorded in Antarctica and the southern oceans. These climate patterns extend to the equatorial Pacific, with pathways along the eastern boundary current system and properties of SAMW being transmitted either directly through eastern boundary upwelling or indirectly via the EUC or via AAIW. Just north of the equatorial front, the climate pattern of near-surface waters shifts to that of the Northern Hemisphere. Remaining puzzles include sorting out the ultimate causes of these dominant northern and southern climate signals. One possibility is that the primary variability is initiated by North Atlantic freshwater anomalies, via thermohaline circulation influence on heat transport and a north-south “see-saw” effect, which is in turn propagated into the South Pacific via intermediate and mode waters (Schmittner et al., 2003) and biogeochemical responses of upper-ocean nutrients (Schmittner, 2005).

**F13.** Stable isotope and Mg/Ca, Site 1242 and Core ME0005A-43JC, p. 56.



Another allows for tropical triggering of climate change, via ENSO dynamics and influences on the hydrologic system (Clement et al., 1999). Another possibility is that the primary variability emanates from the Southern Ocean via transmission through the thermocline circulation to the tropics (Lee and Poulsen, 2006).

## CONCLUSIONS

Leg 202 set sail in 2002 with the goal of probing the climate system at three different scales: tectonic (millions of years), orbital (tens to hundreds of thousands of years, and millennial (thousands of years). In all three time frames, the expedition focused on three goals:

1. Document climate responses to major tectonic and climate events such as uplift of the Andes, closing of the Central American Isthmus, and late Cenozoic expansion of polar ice sheets.
2. Define linkages between high- and low-latitude climate changes in the Southern Hemisphere.
3. Assess the role of biological production and physical ventilation of water masses on the geochemical systems related to oxygen, nutrients, and carbon.

In 4 years of postcruise study, a large group of scientists has made substantial progress toward these goals. Significant results now, that set the stage for further efforts, include establishment and refinement of stratigraphies on all scales.

On the tectonic scales, it appears that the dominant regional response of southeast Pacific eastern boundary current postdates the rise of the Andes prior to 7 Ma. Instead, major cooling occurs roughly synchronously with expansion of polar ice sheets younger than ~3 Ma. The approximate hemispheric symmetry of such cooling implies a global mechanism, such as greenhouse forcing, rather than a purely regional response to Andean uplift. An exception to this finding is that terrigenous dust, most likely from the Atacama Desert, does appear to increase following uplift and then increase further as the ocean cooled.

The primary eastern Pacific response to tectonic closing of the Central American Isthmus is shoaling of the tropical thermocline between 5.3 and 4.0 Ma, followed by significant reduction of sea-surface salinity after 3.7 Ma. We infer that these sequential changes in the eastern Pacific system reflect sequential responses to a gradual (and perhaps not monotonic) restriction of the CAS. The thermocline rise most likely occurred in response to partial restriction, whereas the sea-surface salinity response awaited final closure, when surface waters were no longer able to flow eastward.

On orbital scales, Leg 202 provided dramatic evidence for the growth of 100-k.y. climate cycles during middle Miocene cooling (14.7–12.7 Ma), which in some ways mirrors the reestablishment of similar climate cycles during the MPT (1.2–0.7 Ma). As with the late Pleistocene cycles, greenhouse gas forcing may play a role in the onset and maintenance of these striking climate oscillations.

Within the Pliocene–Pleistocene interval, preliminary results provide some unresolved puzzles in which variability south of the Equator appears to be dominated by 41-k.y. climate cycles related to orbital obliquity, whereas variability north of the Equator tracks 23-k.y. cycles related to orbital precession. One possible scenario is that the SEC is

sensitive to high-latitude climate effects, via regional subsurface circulation and upwelling (the so-called oceanic tunnel effect), whereas the intertropical convergence north of the Equator responds more directly to local insolation, with a precessional rhythm. Firm conclusions on these climate cycles await further data that will confirm the regional patterns of change around the Equator.

Leg 202 provided exciting new materials for study of millennial-scale climate change and provides an unambiguous result that climate oscillations of central Chile tracked changes in Antarctica. This finding refutes past results that suggested climate linkages of Chile to the North Atlantic. Direct correlation of land and marine systems, through terrigenous sediments, iron, and pollen at the ODP sites, shows that some of the terrigenous markers lag the regional marine and polar climate shifts, and this may explain why fragmentary land-based data failed to identify unambiguously the Antarctic climate pattern.

Nitrogen isotope data provide key insights into the biogeochemical system and argue for linkage to the high southern latitudes via subsurface circulation, which influences the oxygen minimum zone off Peru and controls the rate of denitrification in the southeast Pacific.

To be sure, this synthesis can only provide a progress report, rather than final conclusions. Although more than 30 publications have been produced so far, much more research is in progress, and the conclusions we make here may be amplified with greater detail, or modified by new results, as work progresses over the coming decade.

## **ACKNOWLEDGMENTS**

We gratefully acknowledge the hard work and persistence of our shipboard and shore-based scientific colleagues who produced the body of publications describing Leg 202's scientific results that are synthesized here. We are also most grateful to the Leg 202 ship's crew and the marine technicians as well as to our Staff Scientist Peter Blum, who endured stormy seas and extremely trying drilling conditions to accomplish a successful leg. This manuscript has benefited from thoughtful and constructive reviews by Bill Ruddiman, Christina Ravelo, and Chris Poulsen. We also thank Frank Lamy, Heather Benway, Silke Steph, Arne Sturm, and Aysel Sorensen for critical comments, preparation of figures, and editorial help. This research used samples and/or data provided by the Ocean Drilling Program (ODP). ODP is sponsored by the U.S. National Science Foundation (NSF) and participating countries under management of Joint Oceanographic Institutions (JOI, Inc.). Preparation of this synthesis chapter was supported by JOI U.S Science Support Panel (USSSP) and NSF Grants 0319016 and 0426410 (Alan Mix) and through funding from the Deutsche Forschungsgemeinschaft, DFG Grants Ti 240/12 and 13 (Ralf Tiedemann).

## REFERENCES

- Abrantes, F., Lopes, C., Mix, A., and Pisias, N., 2007. Diatoms in southeast Pacific surface sediments reflect environmental properties. *Quat. Sci. Rev.*, 26(1–2):155–169. doi:10.1016/j.quascirev.2006.02.022
- Alley, R.B., Anandkrishnan, S., and Jung, P., 2001. Stochastic resonance in the North Atlantic. *Paleoceanography*, 16(2):190–198. doi:10.1029/2000PA000518
- Anand, P., Elderfield, H., and Conte, M.H., 2003. Calibration of Mg/Ca thermometry in planktonic foraminifera from a sediment trap time series. *Paleoceanography*, 18(2):1050. doi:10.1029/2002PA000846
- Behl, R.J., and Kennett, J.P., 1996. Brief interstadial events in the Santa Barbara Basin, NE Pacific, during the last 60 kyr. *Nature (London, U. K.)*, 379(6562):243–246. doi:10.1038/379243a0
- Bemis, B.E., Spero, H.J., Bijma, J., and Lea, D.W., 1998. Reevaluation of the oxygen isotopic composition of planktonic foraminifera: experimental results and revised paleotemperature equations. *Paleoceanography*, 13(2):150–160. doi:10.1029/98PA00070
- Benway, H.M., Haley, B.A., Klinkhammer, G.P., and Mix, A.C., 2003. Adaptation of a flow-through leaching procedure for Mg/Ca paleothermometry. *Geochem., Geophys., Geosyst.*, 4(2):8403. doi:10.1029/2002GC000312
- Benway, H.M., and Mix, A.C., 2004. Oxygen isotopes, upper-ocean salinity, and precipitation sources in the eastern tropical Pacific. *Earth Planet. Sci. Lett.*, 224(3–4):493–507. doi:10.1016/j.epsl.2004.05.014
- Benway, H.M., Mix, A.C., Haley, B.A., and Klinkhammer, G.P., 2006. Eastern Pacific warm pool paleosalinity and climate variability: 0–30 kyr. *Paleoceanography*, 21(3):PA3008. doi:10.1029/2005PA001208
- Berger, A., Li, X.S., and Loutre, M.F., 1999. Modeling northern hemisphere ice volume over the last 3 Ma. *Quat. Sci. Rev.*, 18(1):1–11. doi:10.1016/S0277-3791(98)00033-X
- Berger, W.H., and Jansen, E., 1994. Mid-Pleistocene climate shift: the Nansen connection. In Overland, J.E., Muench, R.D., and Johannessen, O.M. (Eds.), *The Polar Oceans and their Role in Shaping the Global Environment*. Geophys. Monogr., 85:295–311.
- Berger, W.H., and Wefer, G., 1996. Central themes of South Atlantic circulation. In Wefer, G., Berger, W.H., Siedler, G., and Webb, D.J. (Eds.), *The South Atlantic: Present and Past Circulation*: Berlin (Springer-Verlag), 1–11.
- Billups, K., Ravelo, A.C., Zachos, J.C., and Norris, R.D., 1999. Link between oceanic heat transport, thermohaline circulation, and the Intertropical Convergence Zone in the early Pliocene Atlantic. *Geology*, 27(4):319–322. doi:10.1130/0091-7613(1999)027<0319:LBOHTT>2.3.CO;2
- Blunier, T., and Brook, E.J., 2001. Timing of millennial-scale climate change in Antarctica and Greenland during the last glacial period. *Science*, 291(5501):109–112. doi:10.1126/science.291.5501.109
- Bond, G., Kromer, B., Beer, J., Muscheler, R., Evans, M.N., Showers, W., Hoffmann, S., Lotti-Bond, R., Hajdas, I., and Bonani, G., 2001. Persistent solar influence on North Atlantic climate during the Holocene. *Science*, 294:2130–2136. doi:10.1126/science.1065680
- Bond, G., Showers, W., Cheseby, M., Lotti, R., Almasi, P., deMenocal, P., Priore, P., Cullen, H., Hajdas, I., and Bonani, G., 1997. A pervasive millennial-scale cycle in North Atlantic Holocene and glacial climates. *Science*, 278(5341):1257–1266. doi:10.1126/science.278.5341.1257
- Broecker, W.S., 2006. Was the Younger Dryas triggered by a flood? *Science*, 312(5777):1146–1148. doi:10.1126/science.1123253

- Cacho, I., Ferretti, P., Pena, L., and Shackleton, N., 2006. Last glacial rapid climate variability in surface water properties from the eastern equatorial Pacific Ocean. *Geophys. Res. Abstr.*, 8:09817.
- Calvo, E., Pelejero, C., Herguera, J.C., Palanques, A., and Grimalt, J.O., 2001. Insolation dependence of the southeastern subtropical Pacific sea surface temperature over the last 400 kyrs. *Geophys. Res. Lett.*, 28(12):2481–2484. doi:10.1029/2000GL012024
- Cande, S.C., and Kent, D.V., 1995. Revised calibration of the geomagnetic polarity timescale for the Late Cretaceous and Cenozoic. *J. Geophys. Res.*, 100(B4):6093–6095. doi:10.1029/94JB03098
- Cane, M.A., and Molnar, P., 2001. Closing of the Indonesian Seaway as a precursor to East African aridification around 3–4 million years ago. *Nature (London, U. K.)*, 411(6834):157–162. doi:10.1038/35075500
- Cannariato, K.G., and Ravelo, A.C., 1997. Pliocene–Pleistocene evolution of the eastern tropical Pacific surface water circulation and thermocline depth. *Paleoceanography*, 12(6):805–820. doi:10.1029/97PA02514
- Chaisson, W.P., and Ravelo, A.C., 2000. Pliocene development of the East–West hydrographic gradient in the equatorial Pacific. *Paleoceanography*, 15(5):497–505. doi:10.1029/1999PA000442
- Clark, P.U., Archer, D., Pollard, D., Blum, J.D., Rial, J.A., Brovkin, V., Mix, A.C., Pisias, N.G., and Roy, M., in press. The middle Pleistocene transition: characteristics, mechanisms, and implications for long-term changes in atmospheric pCO<sub>2</sub>. *Quat. Sci. Rev.* doi:10.1016/j.quascirev.2006.07.008
- Clark, P.U., Marshall, S.J., Clarke, G.K.C., Hostetler, S.W., Licciardi, J.M., and Teller, J.T., 2001. Freshwater forcing of abrupt climate change during the last glaciation. *Science*, 293:283–287. doi:10.1126/science.1062517
- Clark, P.U., McCabe, A.M., Mix, A.C., and Weaver, A.J., 2004. Rapid rise of sea level 19,000 years ago and its global implications. *Science*, 304(5674):1141–1144. doi:10.1126/science.1094449
- Clark, P.U., and Mix, A.C., 2002. Ice sheets and sea level of the Last Glacial Maximum. *Quat. Sci. Rev.*, 21(1–3):1–7. doi:10.1016/S0277-3791(01)00118-4
- Clark, P.U., and Pollard, D., 1998. Origin of the middle Pleistocene transition by ice sheet erosion of regolith. *Paleoceanography*, 13(1):1–9. doi:10.1029/97PA02660
- Clement, A.C., Seager, R., and Cane, M.A., 1999. Orbital controls on the El Niño/Southern Oscillation and the tropical climate. *Paleoceanography*, 14(4):441–456. doi:10.1029/1999PA900013
- CLIMAP Project Members, 1981. Seasonal reconstructions of the Earth's surface at the Last Glacial Maximum. *Geol. Soc. Am., Map Chart Ser.*, MC36.
- Collins, L.S., Coates, A.G., Berggren, W.A., Aubry, M.-P., and Zhang, J., 1996. The late Miocene Panama isthmian strait. *Geology*, 24(8):687–690. doi:10.1130/0091-7613(1996)024<0687:TLMPIS>2.3.CO;2
- Crowley, T.J., Kim, K.-Y., Mengel, J.G., and Short, D.A., 1992. Modeling 100,000-year climate fluctuations in pre-Pleistocene time series. *Science*, 255(5045):705–707. doi:10.1126/science.255.5045.705
- Curry, W.B., Shackleton, N.J., Richter, C., et al., 1995. *Proc. ODP, Init. Repts.*, 154: College Station, TX (Ocean Drilling Program). doi:10.2973/odp.proc.ir.154.1995
- De Pol-Holz, R., Ulloa, O., Dezileau, L., Kaiser, J., Lamy, F., and Hebbeln, D., 2006. Melting of the Patagonian ice sheet and deglacial perturbations of the nitrogen cycle in the eastern South Pacific. *Geophys. Res. Lett.*, 33(4):L04704. doi:10.1029/2005GL024477
- Dekens, P.S., Lea, D.W., Pak, D.K., and Spero, H.J., 2002. Core top calibration of Mg/Ca in tropical foraminifera: refining paleotemperature estimation. *Geochem., Geophys., Geosyst.*, 3(4):1022. doi:10.1029/2001GC000200
- Dengo, G., 1985. Tectonic setting for the Pacific margin from southern Mexico to northwestern Columbia. In Naim, A.E., Stehli, F.G., and Uyeda, S. (Eds.), *The Pacific Ocean: The Ocean Basins and Margins*, 7A: New York (Plenum Press), 123–180.

- Denton, G.H., Heusser, C.J., Lowell, T.V., Moreno, P.I., Andersen, B.G., Heusser, L.E., Schlüchter, C., and Marchant, D.R., 1999. Interhemispheric linkage of paleoclimate during the last glaciation. *Geografiska Annaler, Ser. A: Phys. Geogr.*, 81(2):107–153. doi:10.1111/j.0435-3676.1999.00055.x
- Driscoll, N.W., and Haug, G.H., 1998. A short circuit in thermohaline circulation: a cause for Northern Hemisphere glaciation? *Science*, 282(5388):436–438. doi:10.1126/science.282.5388.436
- Duque-Caro, H., 1990. Neogene stratigraphy, paleoceanography and paleobiogeography in northwest South America and the evolution of the Panama seaway. *Palaeogeogr., Palaeoclimatol., Palaeoecol.*, 77(3–4):203–234. doi:10.1016/0031-0182(90)90178-A
- EPICA Community Members, 2004. Eight glacial cycles from an Antarctic ice core. *Nature (London, U. K.)*, 429(6992):623–62. doi:10.1038/nature02599
- Farrell, J.W., Raffi, I., Janecek, T.C., Murray, D.W., Levitan, M., Dadey, K.A., Emeis, K.-C., Lyle, M., Flores, J.-A., and Hovan, S., 1995. Late Neogene sedimentation patterns in the eastern equatorial Pacific Ocean. In Piasias, N.G., Mayer, L.A., Janecek, T.R., Palmer-Julson, A., and van Andel, T.H. (Eds.), *Proc. ODP, Sci. Results*, 138: College Station, TX (Ocean Drilling Program), 717–756. doi:10.2973/odp.proc.sr.138.143.1995
- Feldberg, M.J., and Mix, A.C., 2003. Planktonic foraminifera, sea surface temperatures, and mechanisms of oceanic change in the Peru and south equatorial currents, 0–150 ka BP. *Paleoceanography*, 18(1):1016. doi:10.1029/2001PA000740
- Ganapolski, A., and Rahmstorf, S., 2002. Abrupt glacial climate changes due to stochastic resonance. *Phys. Rev. Lett.*, 88(3):038501. doi:10.1103/PhysRevLett.88.038501
- Garzzone, C.N., Molnar, P., Libarkin, J.C., and MacFadden, B.J., 2006. Rapid late Miocene rise of the Bolivian Altiplano: evidence for removal of mantle lithosphere. *Earth Planet. Sci. Lett.*, 241(3–4):543–556. doi:10.1016/j.epsl.2005.11.026
- Gildor, H., and Tziperman, E., 2001. A sea ice climate switch mechanism for the 100-kyr glacial cycles. *J. Geophys. Res.*, 106(C5):9117–9134. doi:10.1029/1999JC000120
- Gradstein, F.M., Ogg, J.G., and Smith, A. (Eds.), 2004. *A Geologic Time Scale 2004*: Cambridge (Cambridge Univ. Press).
- Gregory-Wodzicki, K.M., 2000. Uplift history of the central and northern Andes: a review. *Geol. Soc. Am. Bull.*, 112(7):1091–1105. doi:10.1130/0016-7606(2000)112<1091:UHOTCA>2.3.CO;2
- Grevemeyer, I., Diaz-Naveas, J.L., Ranero, C.R., Villinger, H.W., and Ocean Drilling Program Leg 202 Scientific Party, 2003. Heat flow over the descending Nazca plate in central Chile, 32°S to 41°S: observations from ODP Leg 202 and the occurrence of natural gas hydrates. *Earth Planet. Sci. Lett.*, 213(3–4):285–298. doi:10.1016/S0012-821X(03)00303-0
- Groottes, P.M., and Stuiver, M., 1997. Oxygen 18/16 variability in Greenland snow and ice with 10<sup>-3</sup>- to 10<sup>5</sup>-year resolution. *J. Geophys. Res.*, 102(C12):26455–26470. doi:10.1029/97JC00880
- Gu, D., and Philander, S.G.H., 1997. Interdecadal climate fluctuations that depend on exchanges between the tropics and extratropics. *Science*, 275(5301):805–807. doi:10.1126/science.275.5301.805
- Harris, S.E., and Mix, A.C., 2002. Climate and tectonic influences on continental erosion in tropical South America, 0–13 Ma. *Geology*, 30(5):447–450. doi:10.1130/0091-7613(2002)030<0447:CATIOC>2.0.CO;2
- Hartley, A.J., 2003. Andean uplift and climate change. *Geol. Soc. Spec. Publ.*, 160:7–10.
- Hartley, A.J., and Chong, G., 2002. Late Pliocene age for the Atacama Desert: implications for the desertification of western South America. *Geology*, 30(1):43–46. doi:10.1130/0091-7613(2002)030<0043:LPAFTA>2.0.CO;2
- Haug, G.H., Ganapolski, A., Sigman, D.M., Rosell-Mele, A., Swann, G.E.A., Tiedemann, R., Jaccard, S.L., Bollmann, J., Maslin, M.A., Leng, M.J., and Eglington, G.,

2005. North Pacific seasonality and the glaciation of North America 2.7 million years ago. *Nature (London, U. K.)*, 433(7028):821–825. doi:10.1038/nature03332
- Haug, G.H., and Tiedemann, R., 1998. Effect of the formation of the Isthmus of Panama on Atlantic Ocean thermohaline circulation. *Nature (London, U. K.)*, 393(6686):673–676. doi:10.1038/31447
- Haug, G.H., Tiedemann, R., Zahn, R., and Ravelo, A.C., 2001. Role of Panama uplift on oceanic freshwater balance. *Geology*, 29(3):207–210. doi:10.1130/0091-7613(2001)029<0207:ROPUOO>2.0.CO;2
- Hay, W.W., 1996. Tectonics and climate. *Geol. Rundsch.*, 85(3):409–437. doi:10.1007/s005310050086
- Haywood, A.M., Dekens, P., Ravelo, A.C., and Williams, M., 2005. Warmer tropics during the mid-Pliocene? Evidence from alkenone paleothermometry and a fully coupled ocean-atmosphere GCM. *Geochem., Geophys., Geosyst.*, 6(3):1–20. doi:10.1029/2004GC000799
- Hendy, I.L., Kennett, J.P., Roark, E.B., and Ingram, B.L., 2002. Apparent synchronicity of submillennial scale climate events between Greenland and Santa Barbara Basin, California from 30–10 ka. *Quat. Sci. Rev.*, 21(10):1167–1184. doi:10.1016/S0277-3791(01)00138-X
- Heusser, L., Heusser, C., Mix, A., and McManus, J., 2006b. Chilean and southeast Pacific paleoclimate variations during the last glacial cycle: directly-correlated pollen and  $\delta^{18}\text{O}$  records from ODP Site 1234. *Quat. Sci. Rev.*, 25(23–24):3404–3415. doi:10.1016/j.quascirev.2006.03.011
- Heusser, L., Heusser, C., and Pisias, N., 2006a. Vegetation and climate dynamics of southern Chile during the past 50,000 years: results of ODP Site 1233 pollen analysis. *Quat. Sci. Rev.*, 25(5–6):474–485. doi:10.1016/j.quascirev.2005.04.009
- Holbourn, A., Kuhnt, W., Schulz, M., and Erlenkeuser, H., 2005. Impacts of orbital forcing and atmospheric carbon dioxide on Miocene ice-sheet expansion. *Nature (London, U. K.)*, 438(7067):483–487. doi:10.1038/nature04123
- Hostetler, S., Pisias, N., and Mix, A., 2006. Sensitivity of Last Glacial Maximum climate to uncertainties in tropical and subtropical ocean temperatures. *Quat. Sci. Rev.*, 25(11–12):1186–1185. doi:10.1016/j.quascirev.2005.12.010
- Hovan, S.A., and Rea, D.K., 1991. Post-Eocene record of Eolian deposition at ODP Site 752, 754, and 756, eastern Indian Ocean. In Weissel, J., Peirce, J., Taylor, E., Alt, J., et al., *Proc. ODP, Sci. Results*, 121: College Station, TX (Ocean Drilling Program), 219–228. doi:10.2973/odp.proc.sr.121.125.1991
- Hulton, N.R.J., Purves, R.S., McCulloch, R.D., Sugden, D.E., and Bentley, M.J., 2002. The Last Glacial Maximum and deglaciation in southern South America. *Quat. Sci. Rev.*, 21(1–3):233–241. doi:10.1016/S0277-3791(01)00103-2
- Imbrie, J., Berger, A., Boyle, E., Clemens, S., Duffy, A., Howard, W., Kukla, G., Kutzbach, J., Martinson, D., McIntyre, A., Mix, A., Molfino, B., Morley, J., Peterson, L., Pisias, N., Prell, W., Raymo, M., Shackleton, N., and Toggweiler, J., 1993. On the structure and origin of major glaciation cycles, 2. The 100,000-year cycle. *Paleoceanography*, 8:699–735.
- Imbrie, J., Boyle, E.A., Clemens, S.C., Duffy, A., Howard, W.R., Kukla, G., Kutzbach, J., Martinson, D.G., McIntyre, A., Mix, A.C., Molfino, B., Morley, J.J., Peterson, L.C., Pisias, N.G., Prell, W.L., Raymo, M.E., Shackleton, N.J., and Toggweiler, J.R., 1992. On the structure and origin of major glaciation cycles, 1. Linear responses to Milankovitch forcing. *Paleoceanography*, 7:701–738.
- Imbrie, J., and Imbrie, J.Z., 1980. Modeling the climatic response to orbital variations. *Science*, 207(4434):943–953. doi:10.1126/science.207.4434.943
- Imbrie, J., McIntyre, A., and Mix, A., 1989. Oceanic response to orbital forcing in the late Quaternary: observational and experimental strategies. In Berger, A., Schneider, S., and Duplessy, J.C. (Eds.), *Climate and the Geosciences*: Dordrecht (Kluwer Academic), 121–164.
- Jousaume, S., Sadourny, R., and Vignal, C., 1986. Origin of precipitating water in a numerical simulation of the July climate. *Ocean-Air Interact.*, 1:43–56.

- Kaiser, J., 2005. Sea-surface temperature variability in the southeast Pacific during the last glacial–interglacial cycle and relationships to paleoenvironmental changes in central and southern Chile [Ph.D. thesis]. Univ. Bremen.
- Kaiser, J., Lamy, F., Arz, H., and Hebbeln, D., in press. Variability of sea surface temperatures off Chile and the dynamics of the Patagonian ice sheet during the last glacial period based on ODP Site 1233. *Quat. Int.*
- Kaiser, J., Lamy, F., and Hebbeln, D., 2005. A 70-kyr sea surface temperature record off southern Chile (Ocean Drilling Program Site 1233). *Paleoceanography*, 20(4):PA4009. doi:10.1029/2005PA001146
- Keigwin, L., 1982. Isotopic paleoceanography of the Caribbean and east Pacific: role of Panama uplift in late Neogene time. *Science*, 217(4557):350–353. doi:10.1126/science.217.4557.350
- Knorr, G., and Lohmann, G., 2003. Southern Ocean origin for the resumption of Atlantic thermohaline circulation during deglaciation. *Nature (London, U. K.)*, 424(6948):532–536. doi:10.1038/nature01855
- Koutavas, A., Lynch-Steiglitz, J., Marchitto, T.M., Jr., and Sachs, J.P., 2002. El Niño-like pattern in ice age tropical Pacific sea surface temperature. *Science*, 297(5579):226–230. doi:10.1126/science.1072376
- Lamy, F., Hebbeln, D., Röhl, U., and Wefer, G., 2001. Holocene rainfall variability in southern Chile: a marine record of latitudinal shifts of the southern westerlies. *Earth Planet. Sci. Lett.*, 185(3–4):369–382. doi:10.1016/S0012-821X(00)00381-2
- Lamy, F., Kaiser, J., Ninnemann, U., Hebbeln, D., Arz, H.W., and Stoner, J., 2004. Antarctic timing of surface water changes off Chile and Patagonian ice sheet response. *Science*, 304(5679):1959–1962. doi:10.1126/science.1097863
- Laskar, J., Joutel, F., and Boudin, F., 1993. Orbital, precessional, and insolation quantities for the Earth from –20 Myr to +10 Myr. *Astron. Astrophys.*, 270:522–533.
- Laskar, J., Robutel, P., Joutel, F., Gastineau, M., Correia, A.C.M., and Levrard, B., 2004. A long-term numerical solution for the insolation quantities of the Earth. *Astron. Astrophys.*, 428(1):261–285. doi:10.1051/0004-6361:20041335
- Lawrence, K.T., Liu, Z., and Herbert, T.D., 2006. Evolution of the eastern tropical Pacific through Plio–Pleistocene glaciation. *Science*, 312(5770):79–83. doi:10.1126/science.1120395
- Lea, D.W., 2004. The 100,000-yr cycle in tropical SST, greenhouse forcing, and climate sensitivity. *J. Climatol.*, 17(11):2170–2179. doi:10.1175/1520-0442(2004)017<2170:TYCITS>2.0.CO;2
- Lea, D.W., Pak, D.K., Belanger, C.L., Spero, H.J., Hall, M.A., and Shackleton, N.J., 2006. Paleoclimate history of Galápagos surface waters over the last 135,000 yr. *Quat. Sci. Rev.*, 25(11–12):1152–1167. doi:10.1016/j.quascirev.2005.11.010
- Lear, C.H., Elderfield, H., and Wilson, P.A., 2000. Cenozoic deep-sea temperatures and global ice volumes from Mg/Ca in benthic foraminiferal calcite. *Science*, 287(5451):269–272. doi:10.1126/science.287.5451.269
- Lee, S.-Y., and Poulsen, C.J., 2005. Tropical Pacific climate response to obliquity forcing in the Pleistocene. *Paleoceanography*, 20(4):PA4010. doi:10.1029/2005PA001161
- Lee, S.-Y., and Poulsen, C.J., 2006. Sea ice control of Plio–Pleistocene tropical Pacific climate evolution. *Earth Planet. Sci. Lett.*, 248(1–2):253–262. doi:10.1016/j.epsl.2006.05.030
- Lisiecki, L.E., and Raymo, M.E., 2005. A Pliocene–Pleistocene stack of 57 globally distributed benthic  $\delta^{18}\text{O}$  records. *Paleoceanography*, 20(1):PA1003. doi:10.1029/2004PA001071
- Liu, Z., and Yang, H., 2003. Extratropical control of tropical climate, the atmospheric bridge and oceanic tunnel. *Geophys. Res. Lett.*, 30(5)1230. doi:10.1029/2002GL016492
- Lourens, L.J., Hilgen, F.J., Laskar, J., Shackleton, N.J., and Wilson, D., 2004. The Neogene period. In Gradstein, F.M., Ogg, J., et al., (Eds.), *A Geologic Time Scale 2004*: Cambridge (Cambridge Univ. Press), 409–440.

- Lowell, T.V., Heusser, C.J., Andersen, B.G., Moreno, P.I., Hauser, A., Heusser, L.E., Schlüchter, C., Marchant, D.R., and Denton, G.H., 1995. Interhemispheric correlation of late Pleistocene glacial events. *Science*, 269(5230):1541–1549. doi:10.1126/science.269.5230.1541
- Lyle, M., Dadey, K.A., and Farrell, J.W., 1995. The late Miocene (11–8 Ma) eastern Pacific carbonate crash: evidence for reorganization of deep-water circulation by the closure of the Panama Gateway. In Piasias, N.G., Mayer, L.A., Janecek, T.R., Palmer-Julson, A., and van Andel, T.H. (Eds.), *Proc. ODP, Sci. Results*, 138: College Station, TX (Ocean Drilling Program), 821–838. doi:10.2973/odp.proc.sr.138.157.1995
- Lynch-Stieglitz, J., 2004. Hemispheric asynchrony of abrupt climate change. *Science*, 304(5679):1919–1920. doi:10.1126/science.1100374
- Maasch, K.A., and Saltzman, B., 1990. A low-order dynamical model of global climatic variability over the full Pleistocene. *J. Geophys. Res.*, 95:1955–1963.
- MacAyeal, D., 1993. Binge/purge oscillations of the Laurentide ice sheet as a cause of the North Atlantic's Heinrich events. *Paleoceanography*, 8(6):775–784.
- Maier-Reimer, E., Mikolajewicz, U., and Crowley, T., 1990. Ocean general circulation model sensitivity experiment with an open Central American isthmus. *Paleoceanography*, 5:349–366.
- Marlow, J.R., Lange, C.B., Wefer, G., and Rosell-Melé, A., 2000. Upwelling intensification as part of the Pliocene–Pleistocene climate transition. *Science*, 290(5500):2288–2291. doi:10.1126/science.290.5500.2288
- Martinez, P., Lamy, F., Robinson, R.R., Pichevin, L., and Billy, I., 2006. Atypical  $\delta^{15}\text{N}$  variations at the southern boundary of the east Pacific oxygen minimum zone over the last 50 ka. *Quat. Sci. Rev.*, 25(21–22):3017–3028. doi:10.1016/j.quascirev.2006.04.009
- McClymont, E.L., and Rosell-Melé, A., 2005. Links between the onset of modern Walker circulation and the mid-Pleistocene climate transition. *Geology*, 33(5):389–392. doi:10.1130/G21292.1
- McManus, J.F., Francois, R., Gherardi, J.-M., Keigwin, L.D., and Brown-Leger, S., 2004. Collapse and rapid resumption of Atlantic meridional circulation linked to deglacial climate changes. *Nature (London, U. K.)*, 428(6985):834–837. doi:10.1038/nature02494
- McManus, J.F., Oppo, D.W., and Cullen, J.L., 1999. A 0.5-million-year record of millennial-scale climate variability in the North Atlantic. *Science*, 283(5404):971–975. doi:10.1126/science.283.5404.971
- Mikolajewicz, U., and Crowley, T.J., 1997. Response of a coupled ocean/energy balance model to restricted flow through the Central American isthmus. *Paleoceanography*, 12(3):429–442. doi:10.1029/96PA03542
- Mix, A.C., 1987. Hundred-kiloyear cycle queried. *Nature (London, U. K.)*, 327(6121):370. doi:10.1038/327370a0
- Mix, A.C., Le, J., and Shackleton, N.J., 1995a. Benthic foraminiferal stable isotope stratigraphy of Site 846: 0–1.8 Ma. In Piasias, N.G., Mayer, L.A., Janecek, T.R., Palmer-Julson, A., and van Andel, T.H. (Eds.), *Proc. ODP, Sci. Results*, 138: College Station, TX (Ocean Drilling Program), 839–854. doi:10.2973/odp.proc.sr.138.160.1995
- Mix, A.C., Lund, D.C., Piasias, N.G., Bodén, P., Bornmalm, L., Lyle, M., and Pike, J., 1999. Rapid climate oscillations in the Northeast Pacific during the last deglaciation reflect Northern and Southern Hemisphere sources. In Webb, R.S., Clark, P.U., and Keigwin, L. (Eds.), *Mechanisms of Millennial-scale Global Climate Change*. Geophys. Monogr., 112:127–148.
- Mix, A.C., Piasias, N.G., Rugh, W., Wilson, J., Morey, A., and Hagelberg, T.K., 1995b. Benthic foraminifer stable isotope record from Site 849 (0–5 Ma): local and global climate changes. In Piasias, N.G., Mayer, L.A., Janecek, T.R., Palmer-Julson, A., and van Andel, T.H. (Eds.), *Proc. ODP, Sci. Results*, 138: College Station, TX (Ocean Drilling Program), 371–412. doi:10.2973/odp.proc.sr.138.120.1995

- Mix, A.C., Tiedemann, R., Blum, P., et al., 2003. *Proc. ODP, Init. Repts.*, 202: College Station, TX (Ocean Drilling Program). doi:10.2973/odp.proc.ir.202.2003
- Molina-Cruz, A., 1977. The relation of the southern trade winds to upwelling processes during the last 75,000 years. *Quat. Res.*, 8:324–339. doi:10.1016/0033-5894(77)90075-8
- Moore, T.C., Jr., 1995. Radiolarian stratigraphy, Leg 138. In Pisias, N.G., Mayer, L.A., Janecek, T.R., Palmer-Julson, A., and van Andel, T.H. (Eds.), *Proc. ODP, Sci. Results*, 138: College Station, TX (Ocean Drilling Program), 191–232. doi:10.2973/odp.proc.sr.138.111.1995
- Moreno, P.I., Jacobson, G.L., Jr., Lowell, T.V., and Denton, G.H., 2001. Interhemispheric climate links revealed by a late-glacial cooling episode in southern Chile. *Nature (London, U. K.)*, 409(6822):804–808. doi:10.1038/35057252
- Mudelsee, M., and Raymo, M.E., 2005. Slow dynamics of the Northern Hemisphere glaciation. *Paleoceanography*, 20(4):PA4022. doi:10.1029/2005PA001153
- Mudelsee, M., and Schulz, M., 1997. The mid-Pleistocene climate transition: onset of 100 ka cycle lags ice volume build-up by 280 ka. *Earth Planet. Sci. Lett.*, 151(1–2):117–123. doi:10.1016/S0012-821X(97)00114-3
- Müller, P.J., Kirst, G., Ruhland, G., von Storch, I., and Rosell-Melé, A., 1998. Calibration of the alkenone paleotemperature index  $U^k_{37}$  based on core-tops from the eastern South Atlantic and the global ocean (60°N–60°S). *Geochim. Cosmochim. Acta*, 62(10):1757–1772. doi:10.1016/S0016-7037(98)00097-0
- Muller, R.A., and MacDonald, G.J., 1997. Glacial cycles and astronomical forcing. *Science*, 277(5323):215–218. doi:10.1126/science.277.5323.215
- Ninnemann, U.S., Kleiven, H., and Euler, C., 2006. Last glacial rapid climate variability in surface water properties from the eastern equatorial Pacific. *Geophys. Res. Abstr.*, 8:09817.
- Nürnberg, D., Müller, A., and Schneider, R.R., 2000. Paleo-sea surface temperature calculations in the equatorial east Atlantic from Mg/Ca ratios in planktic foraminifera: a comparison to sea surface temperature estimates from  $U^k_{37}$ , oxygen isotopes, and foraminiferal transfer function. *Paleoceanography*, 15(1):124–134. doi:10.1029/1999PA000370
- Oppo, D.W., McManus, J.F., and Cullen, J.L., 2003. Paleo-oceanography: deepwater variability in the Holocene epoch. *Nature (London, U. K.)*, 422(6929):277–278. doi:10.1038/422277b
- Ortiz, J.D., O’Connell, S.B., DelViscio, J., Dean, W., Carriquiry, J.D., Marchitto, T., Zheng, Y., and van Geen, A., 2004. Enhanced marine productivity off western North America during warm climate intervals of the past 52 k.y. *Geology*, 32(6):521–524. doi:10.1130/G20234.1
- Paillard, D., 1998. The timing of Pleistocene glaciations from a simple multiple-state climate model. *Nature (London, U. K.)*, 391(6665):378–381. doi:10.1038/34891
- Palmer, M.R., and Pearson, P.N., 2003. A 23,000-year record of surface water pH and  $PCO_2$  in the western equatorial Pacific Ocean. *Science*, 300(5618):80–82. doi:10.1126/science.1080796
- Pena, L.D., Calvo, E., Cacho, I., Eggins, S., and Pelejero, C., 2005. Identification and removal of Mn-Mg-rich contaminant phases on foraminiferal tests: implications for Mg/Ca past temperature reconstructions. *Geochem., Geophys., Geosyst.*, 6(9):Q09P02. doi:10.1029/2005GC000930
- Philander, S.G., and Federov, A.V., 2003. Role of tropics in changing the response to Milankovitch forcing some three million years ago. *Paleoceanography*, 18(2):1045. doi:10.1029/2002PA000837
- Pisias, N.G., Heusser, L., Heusser, C., Hostetler, S.W., Mix, A.C., and Weber, M., 2006. Radiolaria and pollen records from 0 to 50 ka at ODP Site 1233: continental and marine climate records from the Southeast Pacific. *Quat. Sci. Rev.*, 25(5–6):455–473. doi:10.1016/j.quascirev.2005.06.009
- Pisias, N.G., and Mix, A.C., 1997. Spatial and temporal oceanographic variability of the eastern equatorial Pacific during the late Pleistocene: evidence from radiolaria microfossils. *Paleoceanography*, 12(3):381–393. doi:10.1029/97PA00583

- Pisias, N.G., Mix, A.C., and Zahn, R., 1990. Nonlinear response in the global climate system: evidence from benthic oxygen isotopic record in core RC13-110. *Paleoceanography*, 5:147–160.
- Pisias, N.G., and Moore, T.C., Jr., 1981. The evolution of Pleistocene climate: a time series approach. *Earth Planet. Sci. Lett.*, 52(2):450–458. doi:10.1016/0012-821X(81)90197-7
- Pisias, N.G., and Shackleton, N.J., 1984. Modelling the global climate response to orbital forcing and atmospheric carbon dioxide changes. *Nature (London, U. K.)*, 310(5980):757–759. doi:10.1038/310757a0
- Prahl, F.G., Mix, A.C., and Sparrow, M.A., 2006. Alkenone paleothermometry: biological lessons from marine sediment records off western South America. *Geochim. Cosmochim. Acta*, 70(1):101–117. doi:10.1016/j.gca.2005.08.023
- Prange, M., and Schulz, M., 2004. A coastal upwelling seasaw in the Atlantic Ocean as a result of the closure of the Central American seaway. *J. Geophys. Res.*, 31:L17207. doi:10.1029/2004GL020073
- Rahmstorf, S., 1995. Bifurcations of the Atlantic thermohaline circulation in response to changes in the hydrological cycle. *Nature (London, U. K.)*, 378:145–149. doi:10.1038/378145a0
- Rahmstorf, S., 2002. Ocean circulation and climate during the past 120,000 years. *Nature (London, U. K.)*, 419(6903):207–214. doi:10.1038/nature01090
- Ravelo, A.C., Andreasen, D.H., Lyle, M., Lyle, A.O., and Wara, M.W., 2004. Regional climate shifts caused by gradual global cooling in the Pliocene epoch. *Nature (London, U. K.)*, 429(6989):263–267. doi:10.1038/nature02567
- Ravelo, A.C., Dekens, P.S., and McCarthy, M., 2006. Evidence for El Niño-like conditions during the Pliocene. *GSA Today*, 16(3):4–11. doi:10.1130/1052-5173(2006)016<4:EFENLC>2.0.CO;2
- Raymo, M.E., 1997. The timing of major climate terminations. *Paleoceanography*, 12(4):577–585. doi:10.1029/97PA01169
- Raymo, M.E., Oppo, D.W., and Curry, W., 1997. The mid-Pleistocene climate transition: a deep sea carbon isotopic perspective. *Paleoceanography*, 12(4):546–559. doi:10.1029/97PA01019
- Raymo, M.E., and Ruddiman, W.F., 1992. Tectonic forcing of late Cenozoic climate. *Nature (London, U. K.)*, 359:117–122. doi:10.1038/359117a0
- Robinson, R.S., Mix, A., and Martinez, P., 2007. Southern Ocean control on the extent of denitrification in the southeast Pacific over the last 70 ka. *Quat. Sci. Rev.*, 26(1–2):201–212. doi:10.1016/j.quascirev.2006.08.005
- Ruddiman, W.F., 2006. Ice driven CO<sub>2</sub> feedback on ice volume. *Clim. Past*, 2(1):43–55.
- Ruddiman, W.F., and Janecek, T.R., 1989. Pliocene–Pleistocene biogenic and terrigenous fluxes at equatorial Atlantic Sites 662, 663, and 664. In Ruddiman, W., Sarnthein, M., et al., *Proc. ODP, Sci. Results*, 108: College Station, TX (Ocean Drilling Program), 211–240. doi:10.2973/odp.proc.sr.108.165.1989
- Ruddiman, W.F., and Raymo, M.E., 1988. Northern Hemisphere climatic regimes during the past 3 Ma: possible tectonic connections. *Philos. Trans. R. Soc. London, Ser. B*, 318:411–430.
- Sanfilippo, A., and Nigrini, C., 1998. Code numbers for Cenozoic low latitude radiolarian biostratigraphic zones and GPTS conversion tables. *Mar. Micropaleontol.*, 33(1–2):109–117. doi:10.1016/S0377-8398(97)00030-3
- Sarnthein, M., and Fenner, J., 1988. Global wind-induced change of deep-sea sediment budgets, new ocean production and CO<sub>2</sub> reservoirs ca. 3.3–2.35 Ma BP. *Philos. Trans. R. Soc. London*, 318:487–504.
- Sarnthein, M., and Tiedemann, R., 1989. Toward a high-resolution stable isotope stratigraphy of the last 3.4 million years: Sites 658 and 659 off northwest Africa. In Ruddiman, W., Sarnthein, M., et al., *Proc. ODP, Sci. Results*, 108: College Station, TX (Ocean Drilling Program), 167–185. doi:10.2973/odp.proc.sr.108.159.1989
- Scher, H.D., and Martin, E.E., 2006. Timing and climatic consequences of the opening of Drake Passage. *Science*, 312(5772):428–430. doi:10.1126/science.1120044

- Schmidt, M.W., Spero, H.J., and Lea, D.W., 2004. Links between salinity variation in the Caribbean and North Atlantic thermohaline circulation. *Nature (London, U. K.)*, 428(6979):160–163. doi:10.1038/nature02346
- Schmittner, A., 2005. Decline of the marine ecosystem caused by a reduction in the Atlantic overturning circulation. *Nature (London, U. K.)*, 434(7033):628–633. doi:10.1038/nature03476
- Schmittner, A., Saenko, O.A., and Weaver, A.J., 2003. Coupling of the hemispheres in observations and simulations of glacial climate change. *Quat. Sci. Rev.*, 22(5–7):659–671. doi:10.1016/S0277-3791(02)00184-1
- Schneider, B., and Schmittner, A., 2006. Simulating the impact of the Panamanian seaway closure on ocean circulation, marine productivity and nutrient cycling. *Earth Planet. Sci. Lett.*, 246(3–4):367–380. doi:10.1016/j.epsl.2006.04.028
- Schulz, M., Paul, A., and Timmermann, A., 2002. Relaxation oscillators in concert: a framework for climate change at millennial timescales during the late Pleistocene. *Geophys. Res. Lett.*, 29(24):2193. doi:10.1029/2002GL016144
- Shackleton, N.J., 2000. The 100,000-year ice-age cycle identified and found to lag temperature, carbon dioxide, and orbital eccentricity. *Science*, 289(5486):1897–1902. doi:10.1126/science.289.5486.1897
- Shackleton, N.J., Hagelberg, T.K., and Crowhurst, S.J., 1995a. Evaluating the success of astronomical tuning: pitfalls of using coherence as a criterion for assessing pre-Pleistocene timescales. *Paleoceanography*, 10(4):693–698. doi:10.1029/95PA01454
- Shackleton, N.J., and Hall, M.A., 1997. The late Miocene stable isotope record, Site 926. In Shackleton, N.J., Curry, W.B., Richter, C., and Bralower, T.J. (Eds.), *Proc. ODP, Sci. Results*, 154: College Station, TX (Ocean Drilling Program), 367–373. doi:10.2973/odp.proc.sr.154.119.1997
- Shackleton, N.J., Hall, M.A., and Pate, D., 1995b. Pliocene stable isotope stratigraphy of Site 846. In Pisias, N.G., Mayer, L.A., Janecek, T.R., Palmer-Julson, A., and van Andel, T.H. (Eds.), *Proc. ODP, Sci. Results*, 138: College Station, TX (Ocean Drilling Program), 337–355. doi:10.2973/odp.proc.sr.138.117.1995
- Steph, S., 2005. Pliocene stratigraphy and the impact of Panama on changes in Caribbean and tropical east Pacific upper ocean stratification [Ph.D. thesis]. Univ. Kiel.
- Steph, S., Tiedemann, R., Prange, M., Groeneveld, J., Nürnberg, D., Reuning, L., Schulz, M., and Haug, G.H., 2006. Changes in Caribbean surface hydrography during the Pliocene shoaling of the Central American seaway. *Paleoceanography*, 21(4):PA4221. doi:10.1029/2004PA001092
- Stott, L., Poulsen, C., Lund, S., and Thunell, R., 2002. Super ENSO and global climate oscillations at millennial time scales. *Science*, 297(5579):222–226. doi:10.1126/science.1071627
- Thunell, R., Tappa, E., Pride, C., and Kincaid, E., 1999. Sea-surface temperature anomalies associated with the 1997–1998 El Niño recorded in the oxygen isotope composition of planktonic foraminifera. *Geology*, 27(9):843–846. doi:10.1130/0091-7613(1999)027<0843:SSTA AW>2.3.CO;2
- Tiedemann, R., and Franz, S.O., 1997. Deep-water circulation, chemistry, and terrigenous sediment supply in the equatorial Atlantic during the Pliocene, 3.3–2.6 Ma and 5–4.5 Ma. In Shackleton, N.J., Curry, W.B., Richter, C., and Bralower, T.J. (Eds.), *Proc. ODP, Sci. Results*, 154: College Station, TX (Ocean Drilling Program), 299–318. doi:10.2973/odp.proc.sr.154.120.1997
- Tiedemann, R., Sarnthein, M., and Shackleton, N.J., 1994. Astronomic timescale for the Pliocene Atlantic  $\delta^{18}\text{O}$  and dust flux records of Ocean Drilling Program Site 659. *Paleoceanography*, 9(4):619–638. doi:10.1029/94PA00208
- Tziperman, E., and Gildor, H., 2003. On the mid-Pleistocene transition to 100-kyr glacial cycles and the asymmetry between glaciation and deglaciation times. *Paleoceanography*, 18(1):1001. doi:10.1029/2001PA000627
- Visser, K., Thunell, R., and Stott, L., 2003. Magnitude and timing of temperature change in the Indo-Pacific warm pool during deglaciation. *Nature (London, U. K.)*, 421(6919):152–155. doi:10.1038/nature01297

- Voelker, A.H.L., 2002. Global distribution of centennial-scale records for marine isotope stage (MIS) 3: a database. *Quat. Sci. Rev.*, 21(10):1185–1212. doi:10.1016/S0277-3791(01)00139-1
- Waelbroeck, C., Labeyrie, L., Michel, E., Duplessy, J.C., McManus, J.F., Lambeck, K., Balbon, E., and Labracherie, M., 2002. Sea-level and deep water temperature changes derived from benthic foraminifera isotopic records. *Quat. Sci. Rev.*, 21(1–3):295–305. doi:10.1016/S0277-3791(01)00101-9
- Wara, M.W., Ravelo, A.C., and Delaney, M.L., 2005. Permanent El Niño-like conditions during the Pliocene warm period. *Science*, 309(5735):758–761. doi:10.1126/science.1112596
- Weaver, A.J., Saenko, O.A., Clark, P.U., and Mitrovica, J.X., 2003. Meltwater pulse 1A from Antarctica as a trigger of the Bølling-Allerød warm interval. *Science*, 299(5613):1709–1713. doi:10.1126/science.1081002
- Weyl, P.K., 1968. The role of the oceans in climatic change: a theory of the ice ages. *Meteorol. Monogr.*, 8:37–62.
- Zachos, J., Pagani, M., Sloan, L., Thomas, E., and Billups, K., 2001. Trends, rhythms, and aberrations in global climate 65 Ma to present. *Science*, 292(5517):686–693. doi:10.1126/science.1059412
- Zaucker, F., Stocker, T.F., and Broecker, W.S., 1994. Atmospheric freshwater fluxes and their effect on the global thermohaline circulation. *J. Geophys. Res.*, 99(C6):12443–12458. doi:10.1029/94JC00526

Figure F1. Site locations of Leg 202. Site 1232 is in the Chile Basin; Sites 1233–1235 are on the Chile margin; Sites 1236 and 1237 are on Nazca Ridge; Sites 1238 and 1239 are on Carnegie Ridge; Site 1240 is in the Panama Basin; and Sites 1241 and 1242 are on Cocos Ridge.

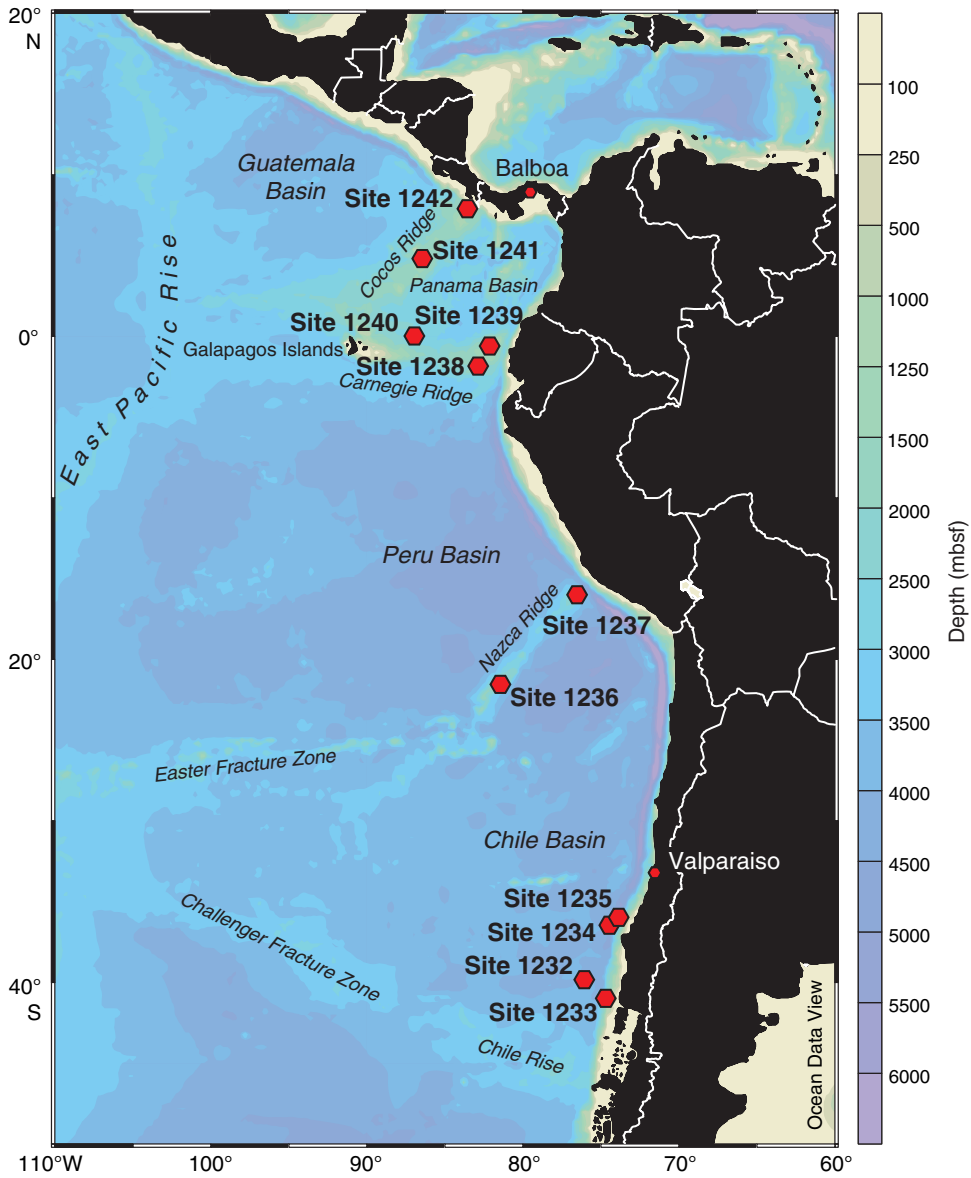
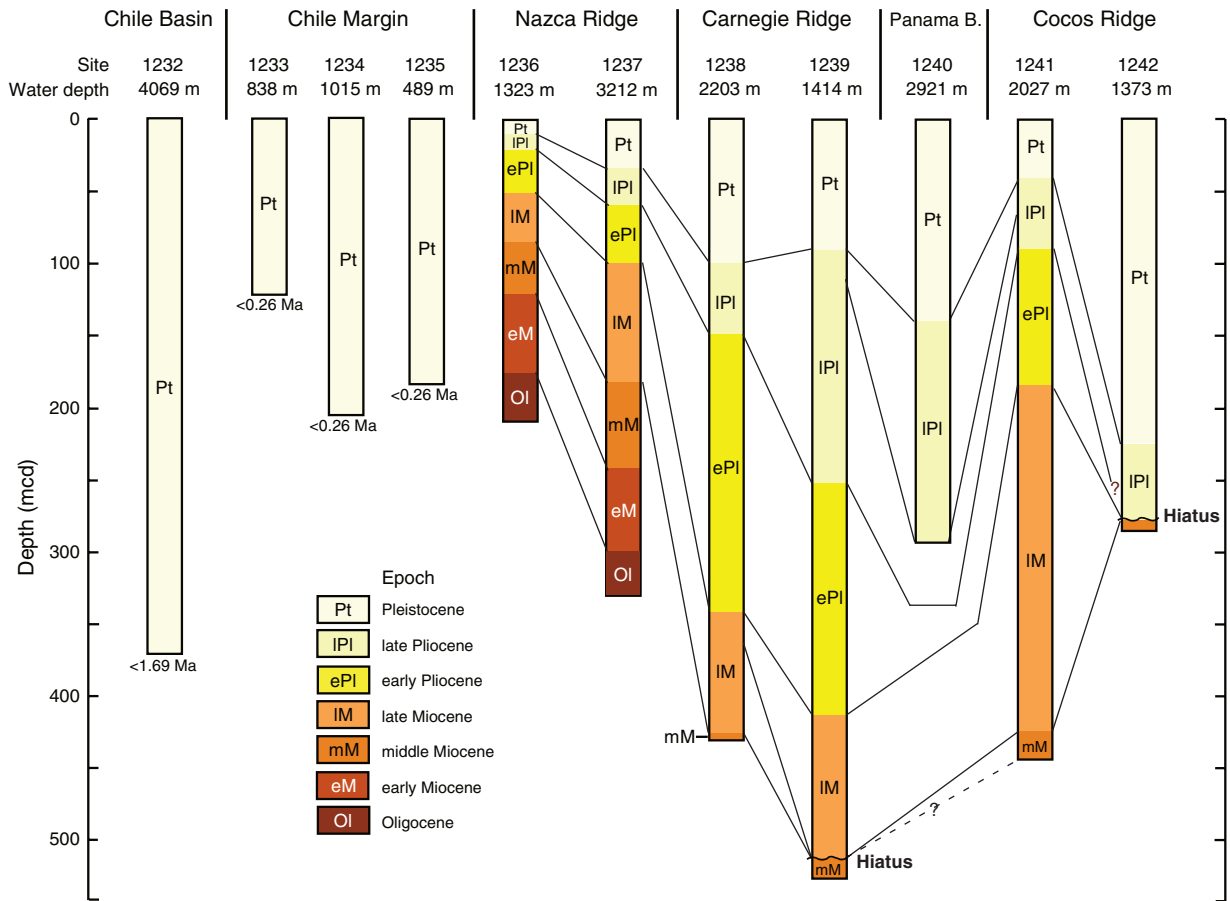
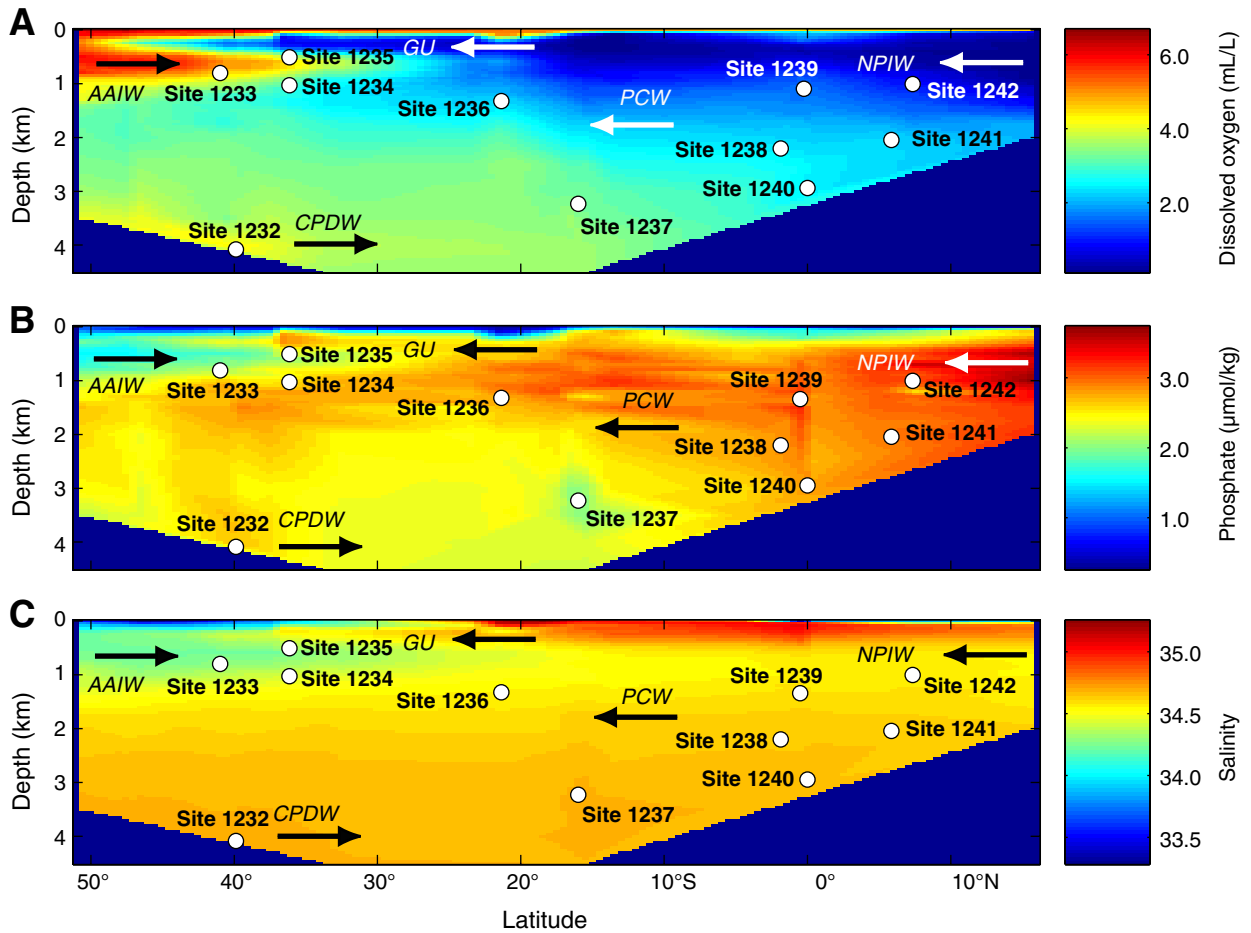


Figure F2. Summary stratigraphic columns document cored intervals, ages, and water depths at Sites 1232–1242. B. = Basin.



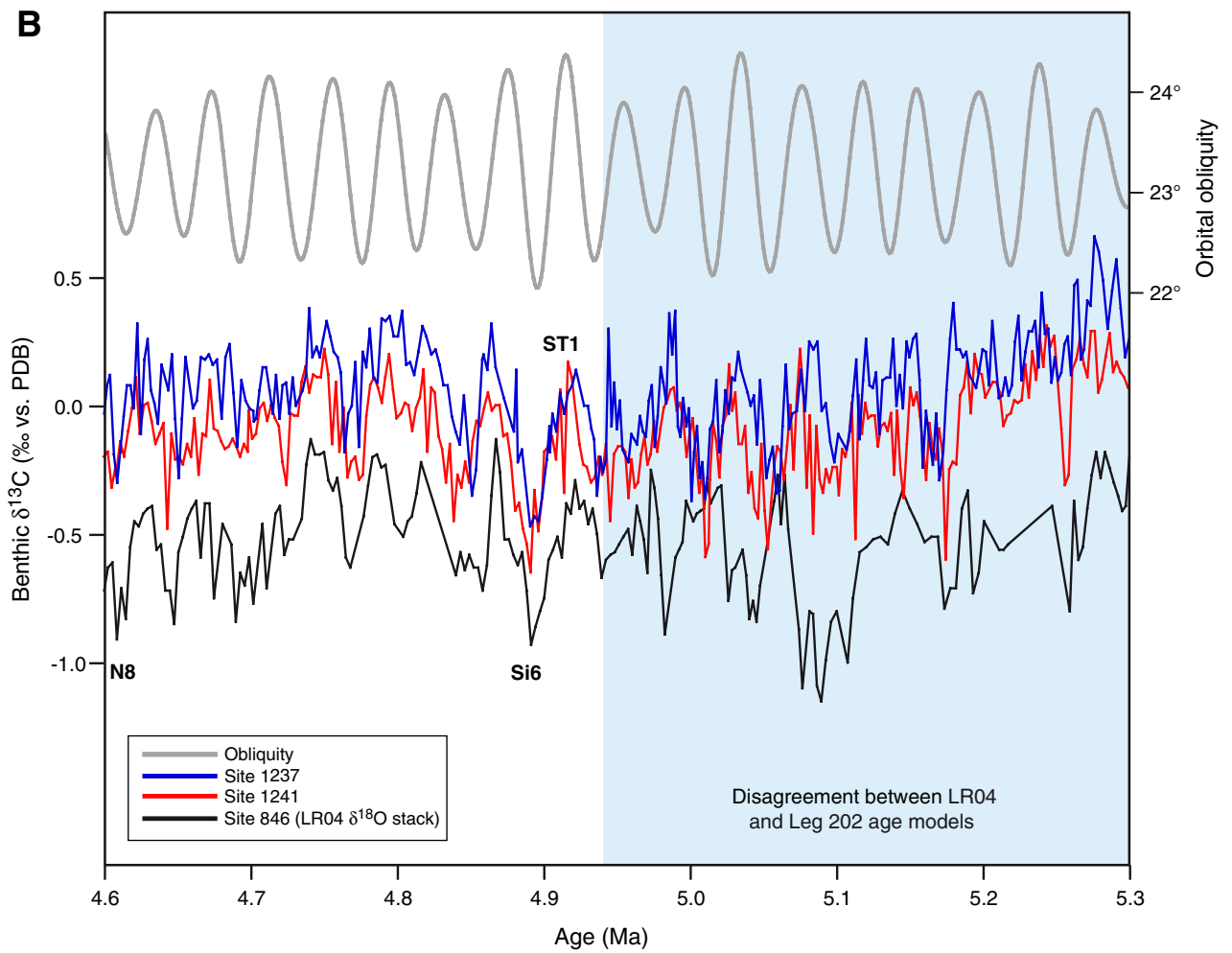
**Figure F3.** Cross section of subsurface water masses in a transect through the drilling sites, characterized by (A) dissolved oxygen, (B) dissolved phosphate, and (C) salinity. AAIW = Antarctic Intermediate Water, NPIW = North Pacific Intermediate Water, PCW = Pacific Central Water, GUC = Gunther Undercurrent, CPDW = Circumpolar Deep Water.



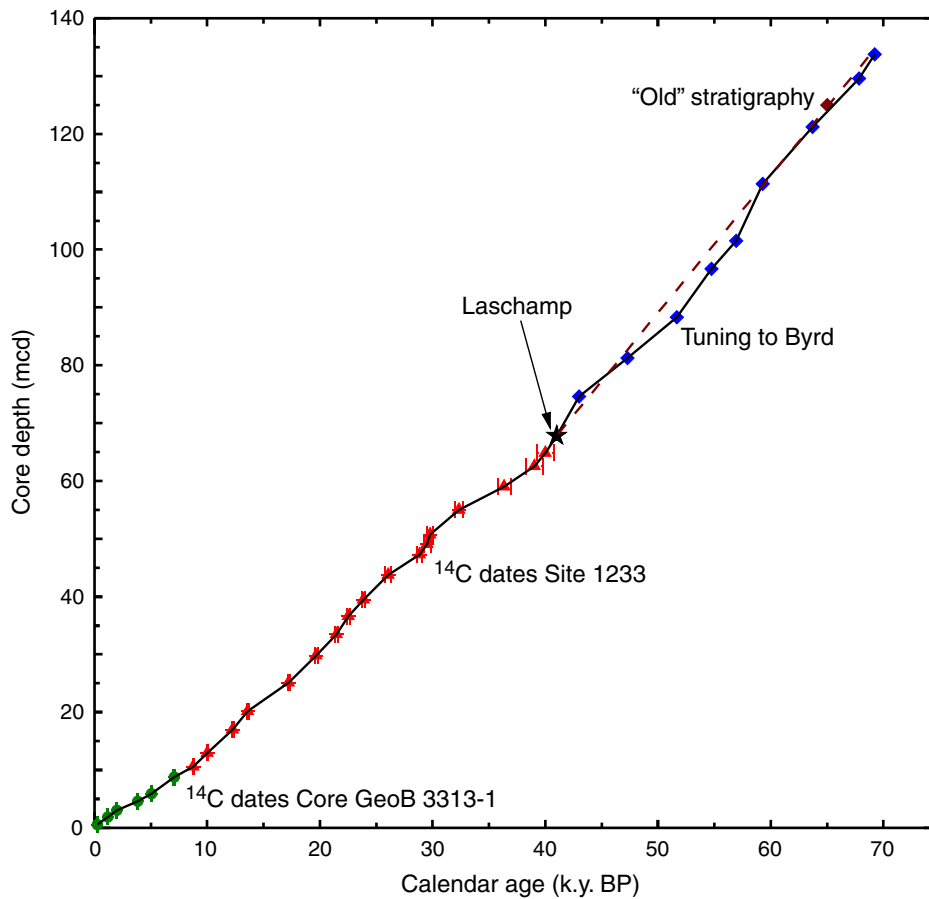
**Figure F4. A.** Example of integrating radiolarian-, magneto-, and isotope-stratigraphy on the basis of an orbitally tuned timescale for the time interval from 2.4 to 6 Ma (Weber and Pisias, this volume; Tiedemann et al., this volume). The benthic  $\delta^{18}\text{O}$  stack of Lisiecki and Raymo (2005), which is also based on an orbitally tuned age model (LR04), is shown for comparison. The chronologies of assigned oxygen isotope stages between Leg 202 records and the  $\delta^{18}\text{O}$ -LR04 stack agree within their error ranges of a few thousand years, except for the time interval older than 4.9 Ma, where the structure of Leg 202 isotope stages deviate from those presented by Lisiecki and Raymo (2005). Oxygen and carbon isotope stages are numbered following the numbering scheme of Shackleton et al. (1995a), which is firmly linked to the underlying 41-k.y. isotope cycles. Even numbers indicate cold stages and odd numbers indicate warm stages. Letters in front of marine isotope stages identify the magnetic polarity interval. For example, the first cold stage of the Sidufjall Chron is called Si2 and the first cold stage occurring in the magnetic interval between the Sidufjall and Thvera is called ST2. FO = first occurrence, LO = last occurrence. PDB = Peedee belemnite. (Figure shown on next page.)



Figure F4 (continued). B. Records of orbital obliquity and  $\delta^{13}\text{C}$  from Sites 1237 and 1240 in comparison with the  $\delta^{13}\text{C}$  record from Site 846, which was one of the key records used to create the LR04  $\delta^{18}\text{O}$  stack (see A). The two age models deviate from each other prior to 4.9 Ma.



**Figure F5.** Age model of the 135.7-mcd-long composite sequence at Site 1233 covering the last ~70 k.y. as published in Lamy et al. (2004) and Kaiser et al. (2005). The uppermost ~9 mcd has been correlated to the AMS  $^{14}\text{C}$  dated gravity Core GeoB 3313-1 from the same location (Lamy et al., 2001). Age control for the ~10- to ~70-mcd interval is provided by 17 AMS  $^{14}\text{C}$  dates on mixed planktonic foraminifer samples and the record of the Laschamp magnetic field excursion (Lund et al., this volume b). All AMS  $^{14}\text{C}$  dates were calibrated with CALPAL software using the CALPAL 2004 January calibration curve ([www.calpal.de](http://www.calpal.de)). Downcore, the initial stratigraphy ("old" stratigraphy as in Lamy et al., 2004) was based on a preliminary definition of MIS 4.2. The age model of this interval was refined by tuning to the Byrd ice-core oxygen isotope record (Blunier and Brook, 2001), as published in Kaiser et al., 2005.



**Figure F6.** Summary of late Cenozoic  $\delta^{18}\text{O}$  climate evolution, major tectonic events, and changes in polar ice volume (modified from Zachos et al., 2001). Studies on orbital-scale climate variability by Steph et al. (this volume), Groeneveld et al. (this volume), Tiedemann et al. (this volume), and Holbourn et al. (2005) considered the highlighted time intervals. Modifications to the figure of Zachos et al. (2001): first occurrence of ash layers at Site 1237 (~9 Ma) and frequency of ash layers according to Mix, Tiedemann, Blum, et al. (2003); uplift of the Andes (Gregory-Wodzicki, 2000), aridification of the Atacama Desert (Hartley, 2003), closure history of the Central American Seaway (CAS, Haug and Tiedemann, 1998); timing for the opening of the Drake Passage (Scher and Martin, 2006). FO = first occurrence.

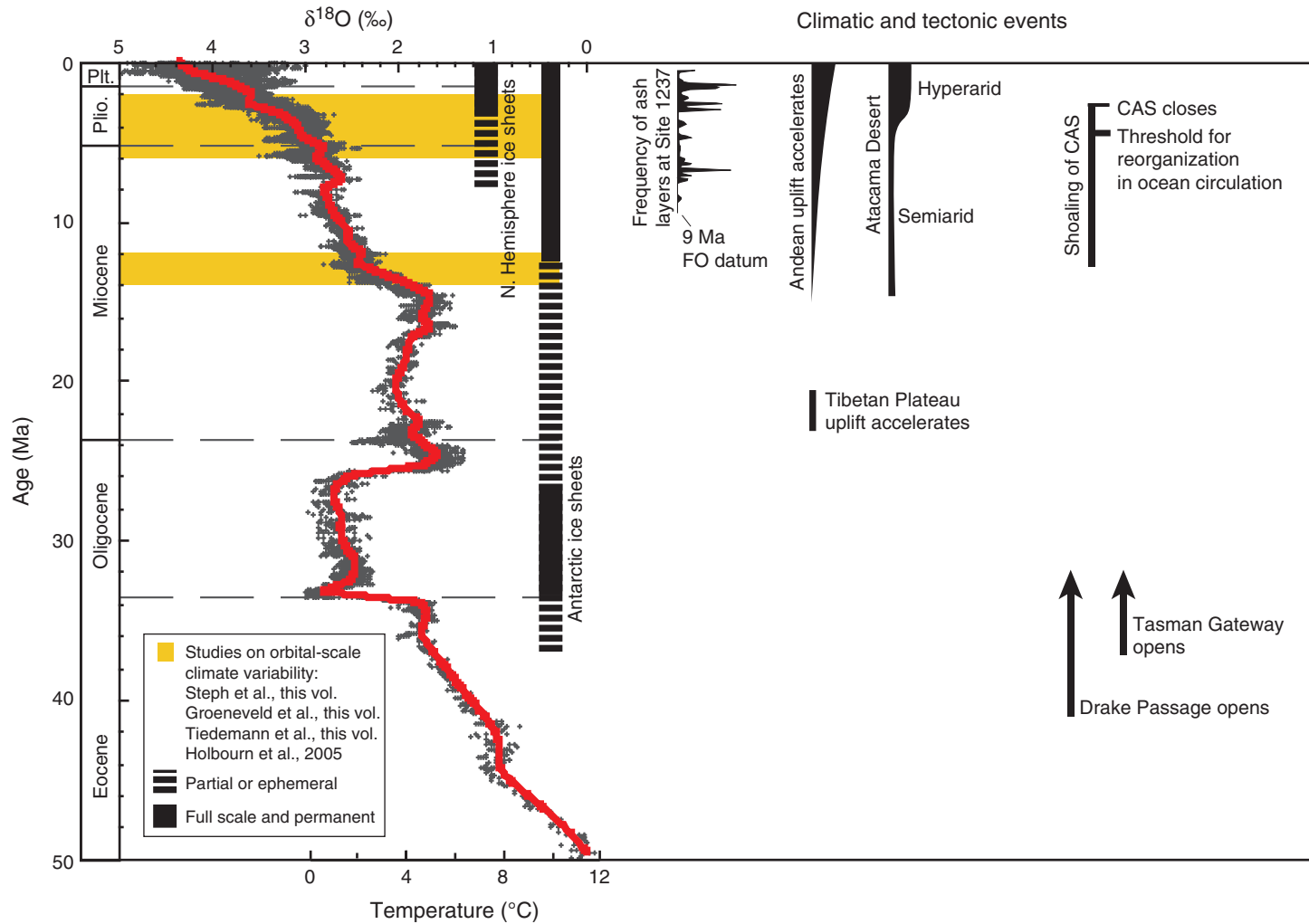


**Figure F7.** Plate tectonic backtrack of Leg 202 and Leg 138 drill sites (Mix, Tiedemann, Blum, et al., 2003). Large circles = modern location, successive circles = backtrack position relative to South America ( $t = 1\text{-m.y.}$  intervals). EQ = Equator, NECC = North Equatorial Counter Current, EUC = Equatorial Undercurrent, SEC = South Equatorial Current, HC = Humboldt Current, SST = sea-surface temperature.

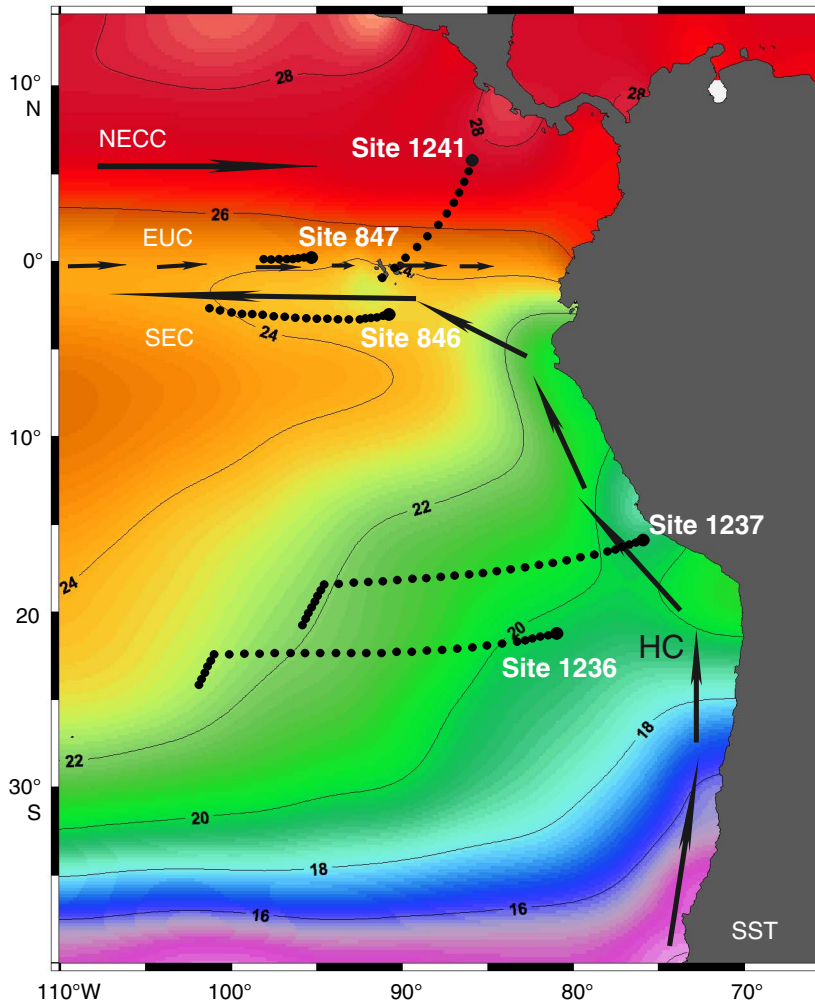
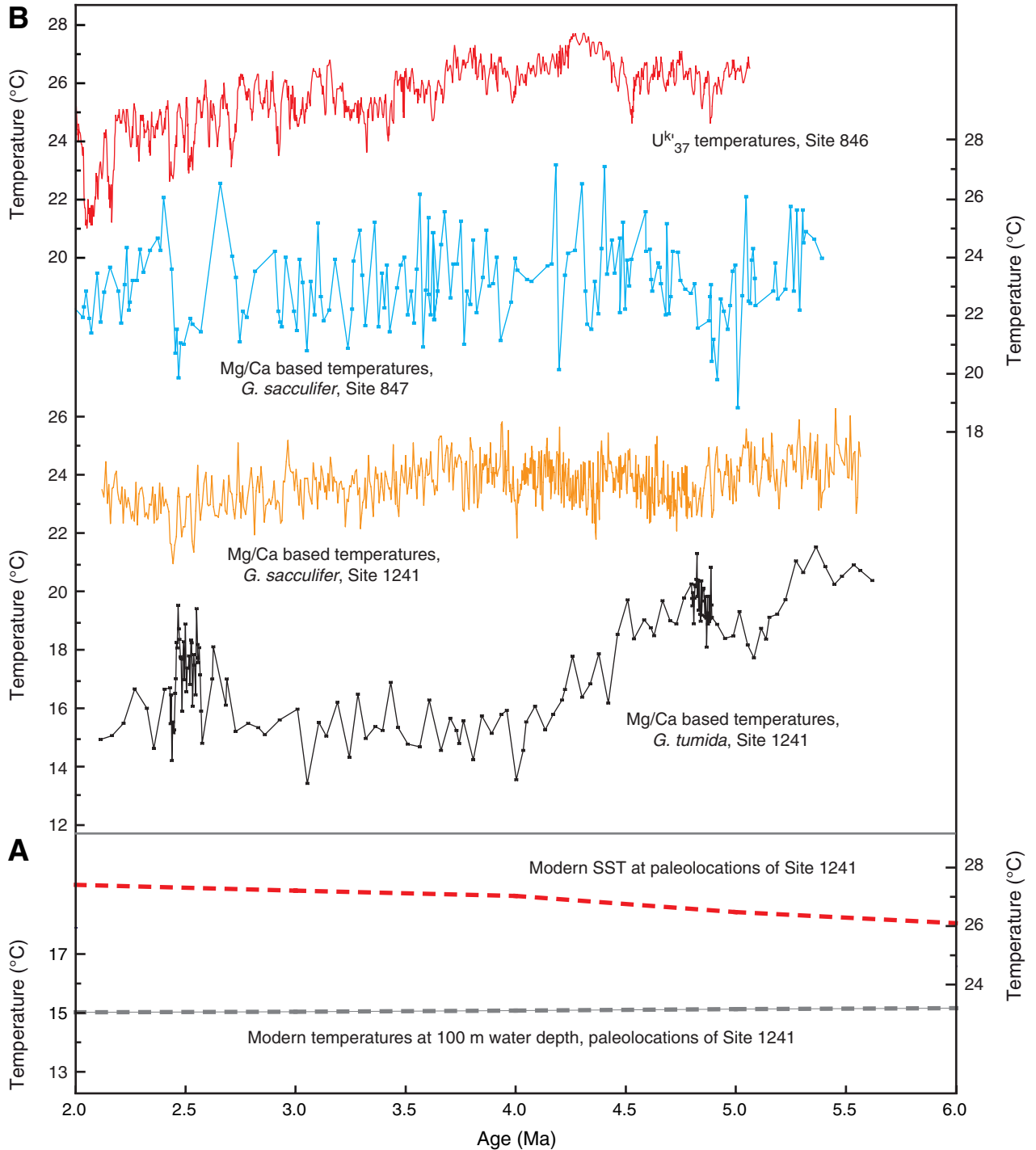
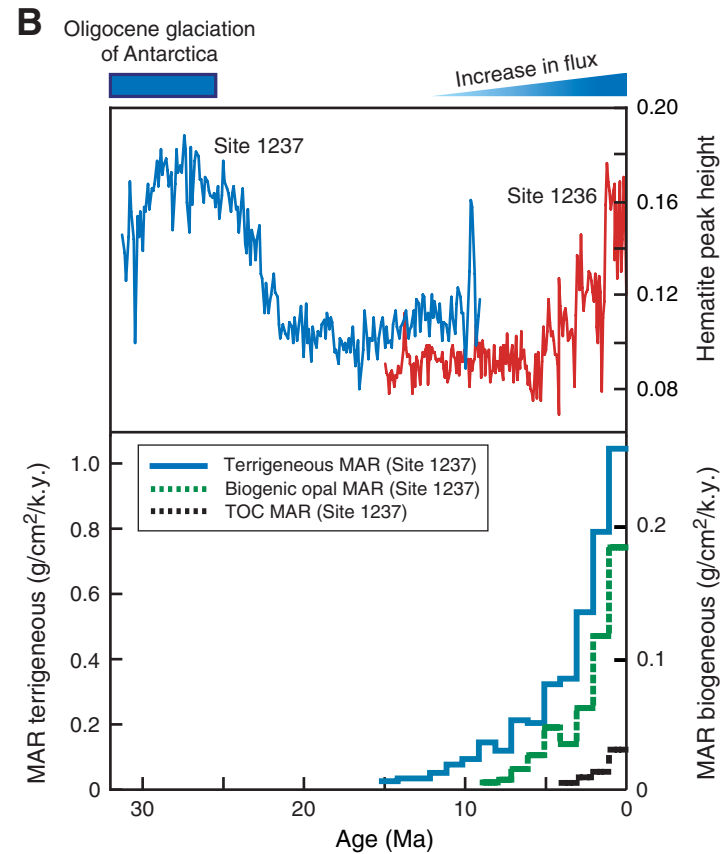
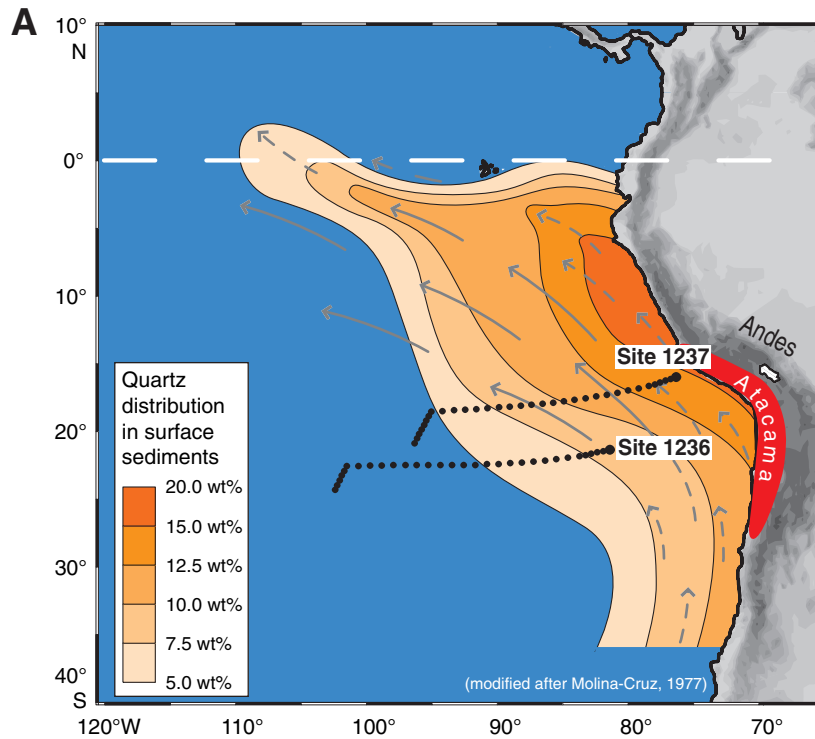


Figure F8. A. Modern annual-average temperatures at 0 and 100 m water depth at paleolocations of Site 1241, based on plate tectonic backtracking and the assumption of no temporal changes in regional oceanic properties since today (Mix, Tiedemann, Blum, et al., 2003). B. Planktonic Mg/Ca temperature reconstructions from the mixed-layer-dweller *G. sacculifer* and the deep-dweller *G. tumida* at Site 1241 (Groeneveld et al., this volume; Steph et al., this volume). Reconstructed alkenone-based SSTs from Site 846 (Lawrence et al., 2006) and planktonic Mg/Ca-derived temperatures (*G. sacculifer*) from Site 847 (Wara et al., 2005) are shown for comparison.



**Figure F9.** A. Quartz distribution in surface sediments of the subtropical southeast Pacific, expressed as weight percentage (carbonate- and opal-free basis, reproduced from Molina-Cruz, 1977). Arrows indicate trade winds. Sites 1236 and 1237 are shown with their plate tectonic backtracks. B. Hematite peak height at Sites 1236 and 1237. The hematite peak height is derived from color reflectance spectra and serves as a proxy for changing concentrations of hematite. Mass accumulation rates (MAR) of total organic carbon (TOC), biogenic opal, and terrigenous material (terrigenous MAR was estimated as  $100\% - \text{wt}\% \text{ CaCO}_3 - \text{wt}\% \text{ organic matter} - \text{wt}\% \text{ biogenic opal} / \text{sedimentation rate dry bulk density}$ ). Shipboard magnetostratigraphy and biostratigraphy were used to calculate sedimentation rates that were smoothed to avoid overinterpretations of the preliminary age model. Terrigenous MAR is used as a proxy for dust flux; biogenic opal and TOC MAR are used as a proxy for paleoproductivity.



**Figure F10. A.** Modern annual-average SST at paleolocations of Site 1237, based on plate tectonic backtracking and the assumption of no temporal changes in regional oceanic properties (Mix, Tiedemann, Blum, et al., 2003). **B.** Planktonic Mg/Ca temperature reconstructions from the mixed-layer-dweller *G. sacculifer* (Wara and Ravelo, this volume) and alkenone-derived  $U^{k}_{37}$  SSTs (Abe et al., this volume; Prahl et al., 2006) for the last 6 m.y. at the position of Site 1237.  $U^{k}_{37}$  SSTs from Sites 958 (off the coast of northwest Africa) and 1084 (Benguela upwelling system) are shown for comparison (Marlow et al., 2000).

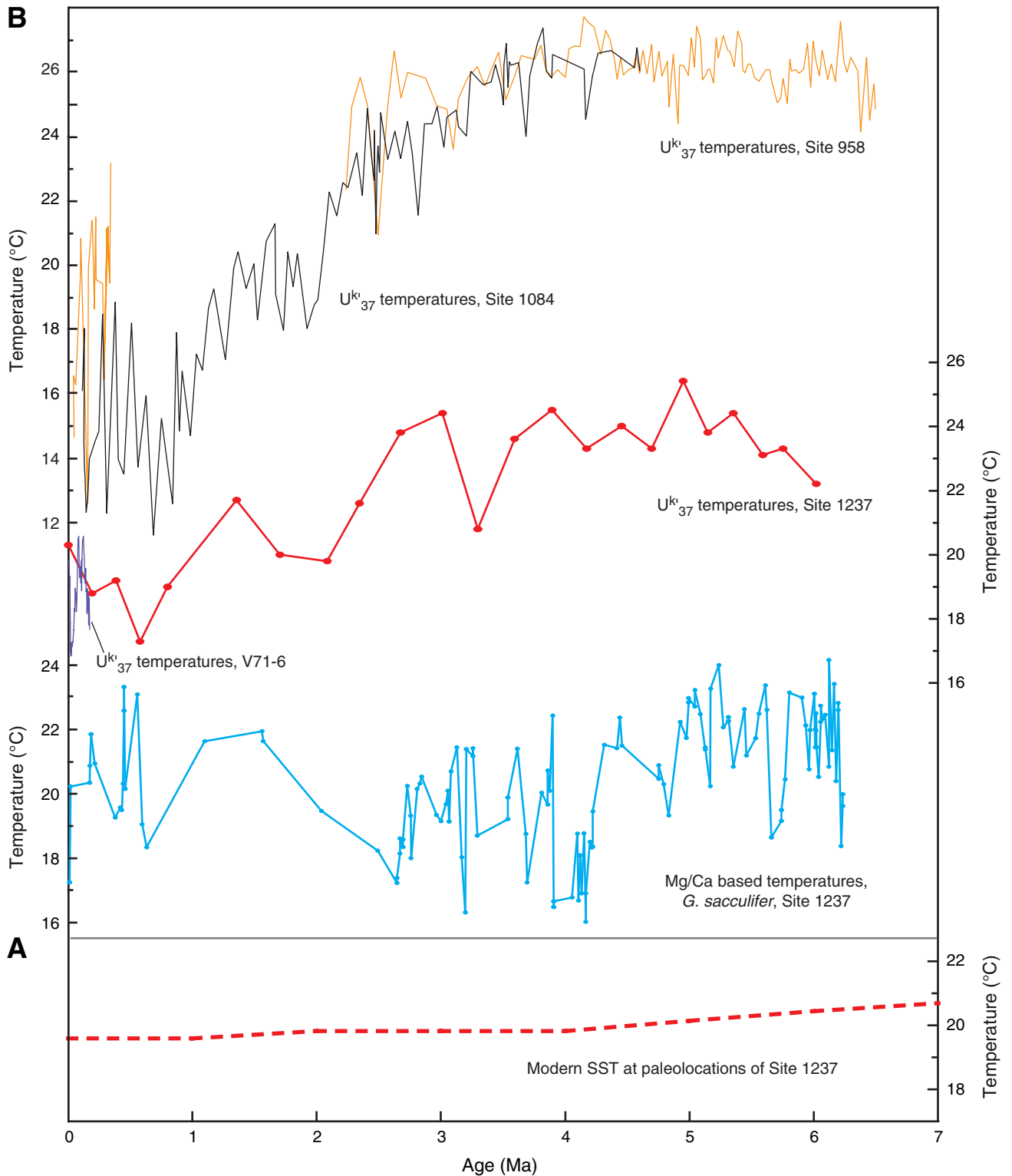


Figure F11. A. Map of millennial-scale sites and surface currents at equatorial Sites 1240 and 1242. NECC = North Equatorial Countercurrent, EUC = Equatorial Undercurrent, SEC = South Equatorial Current, CC = Columbian Current, PCC = Peru Chile Current, PCCC = Peru Chile Countercurrent, GU = Gunther Undercurrent, CFW = Chilean Fjord Water, ACC = Antarctic Circumpolar Current. (Continued on next page.)

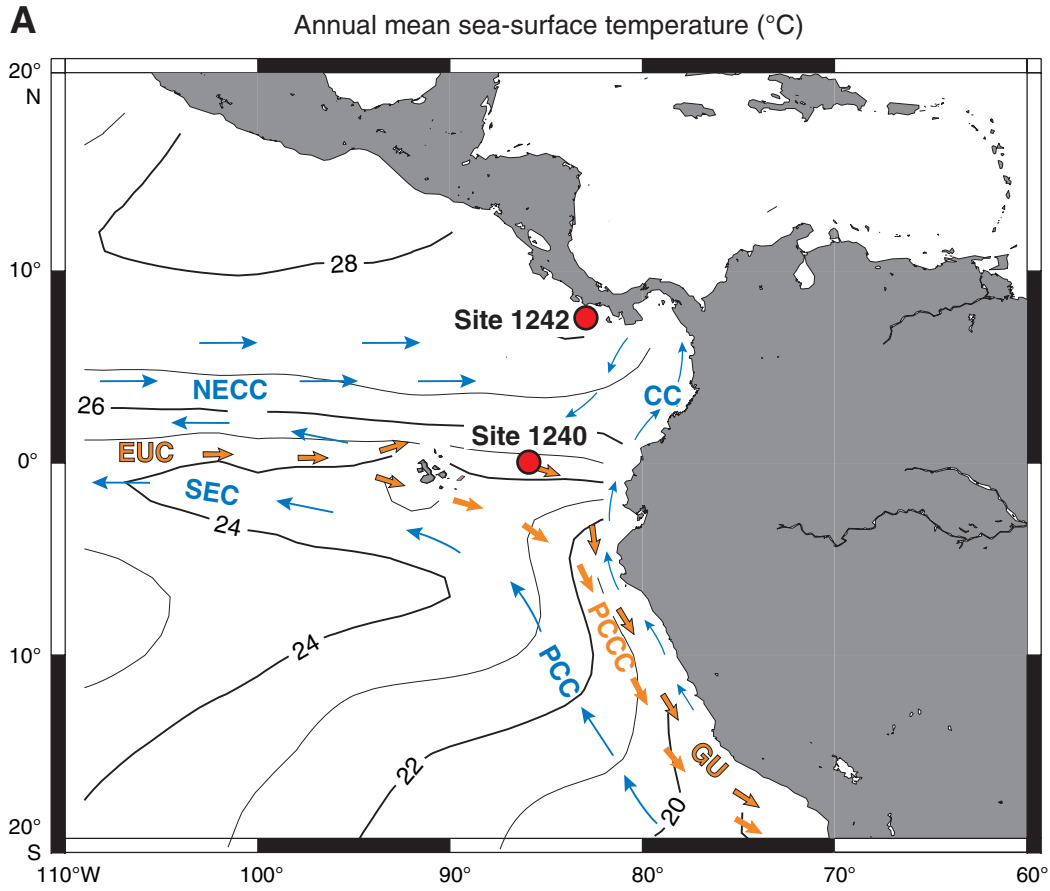
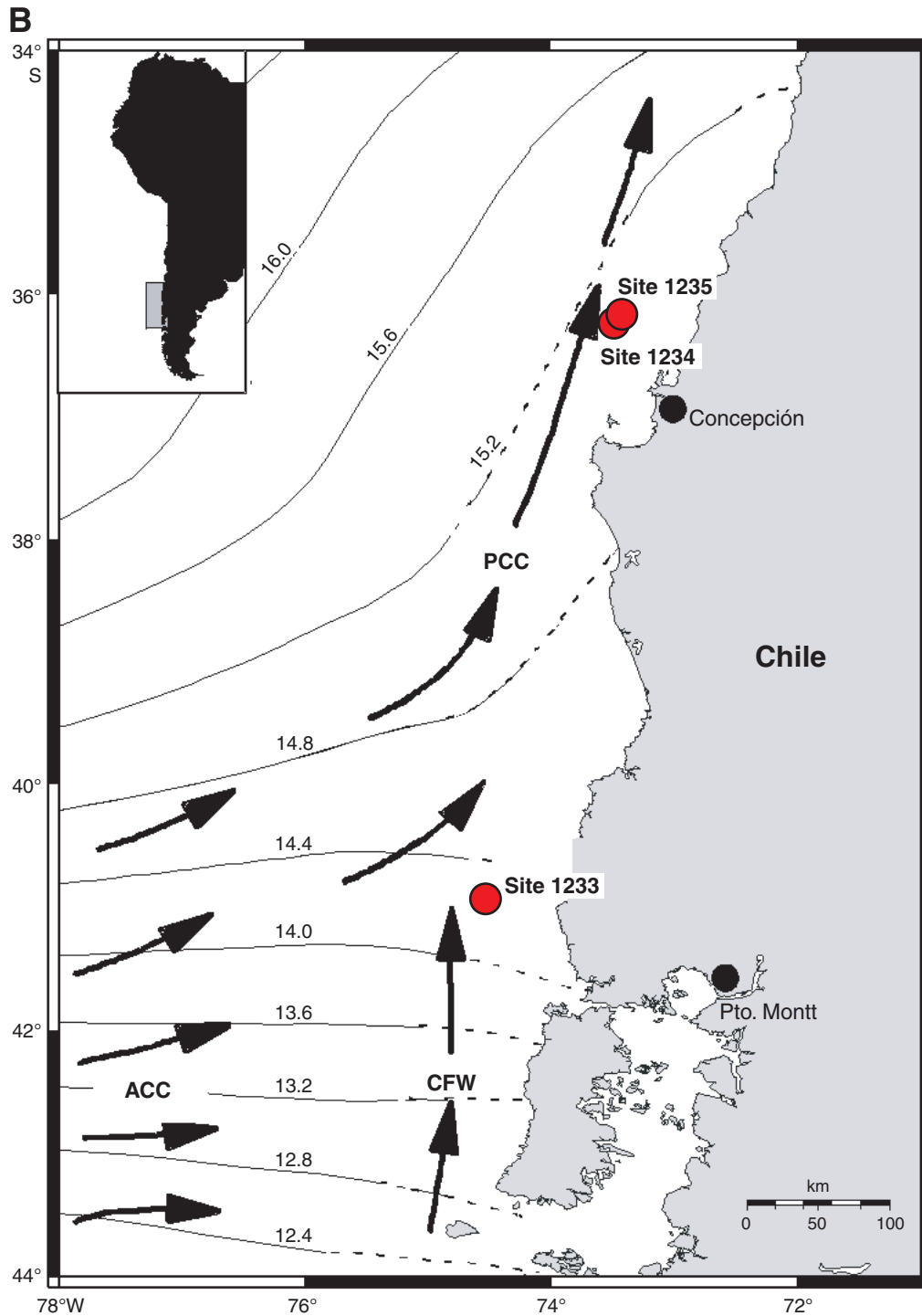
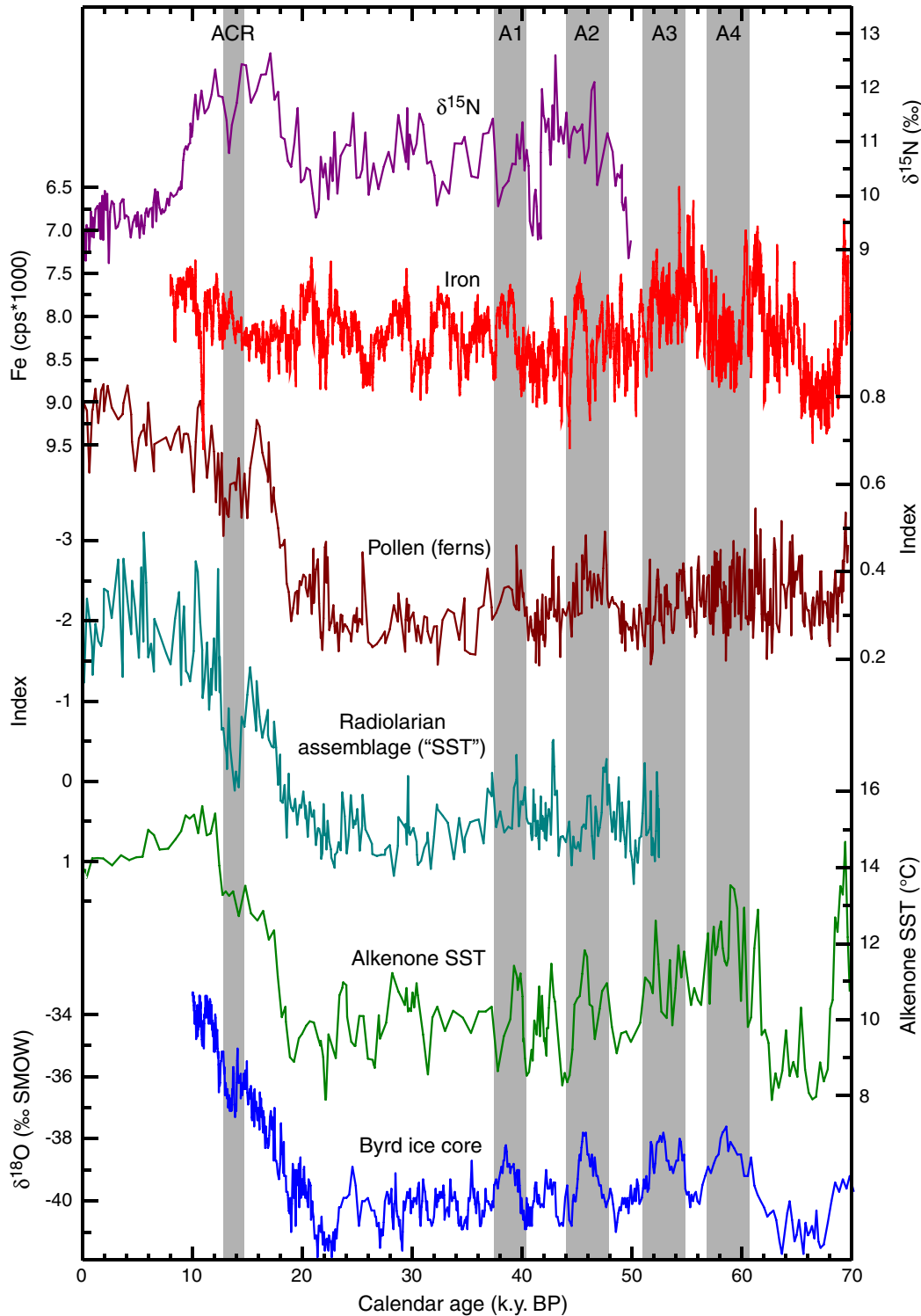


Figure F11 (continued). B. Map of millennial-scale sites and surface currents at southern Chile Sites 1233, 1234, and 1235.



**Figure F12.** Comparison of different proxy records from Site 1233 to the Antarctic climate record from the Byrd ice core: nitrogen isotope record (Martinez et al., 2006), iron content record as a proxy for the extent of the Patagonian ice sheet (Lamy et al., 2004; Kaiser et al., in press), exemplary pollen record (ferns) recording terrestrial climate change (Heusser et al., 2006b), first canonical variates from radiolarian multivariate data sets used as a proxy for sea-surface temperatures (SSTs) (Pisias et al., 2006), alkenone SSTs (Lamy et al., 2004; Kaiser et al., 2005), and oxygen isotope record from the Byrd ice core (Blunier and Brook, 2001) as a proxy for temperature changes over Antarctica. SMOW = Standard Mean Ocean Water. ACR = Antarctic Cold Reversal. A1, A2, A3, A4 = Antarctic Cold Reversal sub-events.



**Figure F13.** Stable isotope and Mg/Ca data from Site 1242 (open symbols), and site survey Core ME0005A-43JC (solid symbols, data from Benway et al., 2006).  $\delta^{18}\text{O}_c$  of planktonic foraminifer *G. ruber*. Mg/Ca-based temperature estimates for *G. ruber*: Mg/Ca was analyzed using the method of Benway et al. (2003) and converted to temperature using  $\text{Mg/Ca} = 0.38\text{Exp}(0.090T)$  (Anand et al., 2003).  $\delta^{18}\text{O}_{\text{sw}}$  estimates calculated from *G. ruber* Mg/Ca and  $\delta^{18}\text{O}_c$  (Bemis et al., 1998; Thunell et al., 1999) and corrected for ice volume (IV) changes (Clark and Mix, 2002; Waelbroeck et al., 2002): solid line = scaling of 0.01‰/m, dashed line = scaling of 0.0075‰/m decrease in relative sea level. For the combined records of the two sites a Gaussian smoothing function (time step = 0.2 k.y.; filter width = 0.8 k.y.) was applied. Calendar-corrected radiocarbon dates are shown with  $\pm 1\sigma$  error bars. GISP2  $\delta^{18}\text{O}_{\text{ice}}$  (Grootes and Stuiver, 1997), indicating high-latitude air temperatures: cold (blue bars) and warm (or sea level rise) events (red bars) of the last 30 k.y. are indicated. 8.2 ka cold event; YD = Younger Dryas cold event; BA = Bølling-Allerød cold event, H1, H2, H3 = Heinrich events; 19 ka = earliest postglacial sea level rise. VSMOW = Vienna Standard Mean Ocean Water, VPDB = Vienna Pee Dee belemnite.

